Cigarette smoke exposure sets up a pro-inflammatory circuit in the lung that induces the hyper-activation of myelin-specific T helper cells

Nuria Alvarez-Sanchez*[1,2], Annette Haughian*[1], Brendan Cordeiro*[1,2], Elvira Paneda[3], Thomas A. Heaney[2,6], Molly Pitkethly[1], Jhenifer Gabriela Vasquez Rojas[1,3], Emily Pullen[6], Elyse Latreille[1], Warren L. Lee[1], Martin Stampfli[5], Clinton Robbins[2,3], Shannon E. Dunn[2,3,4,6]

[1]Keenan Research Center of St. Michael's Hospital, Toronto, ON, Canada

[2]Department of Immunology, University of Toronto, Toronto, ON, Canada

[3]Toronto General Hospital Research Institute, Toronto, ON, Canada

[4]Women's College Research Institute, Toronto, ON, Canada

[5]Department of Pathology and Molecular Medicine, McMaster University, Hamilton, ON, Canada

[6]Sunnybrook Research Institute, Toronto, ON, Canada

*co-first authors

Corresponding author: Shannon E. Dunn, Sunnybrook Research Institute, Toronto, ON, Canada

Author contributions: N.A-S, A.H. and B.C. conceived and conducted experiments, analyzed data, and drafted the manuscript. Elvira Paneda conducted smoke and ambient air exposures on mice. M.P. and E. Pullen conducted histological analysis of CNS in EAE studies. J.V.R. conducted clinical scoring on some EAE studies. E.L. and W.L.L helped with lung studies. T.H. conducted human ELISPOTs. M.S. and C.R. designed the smoking paradigm and helped obtain funding for the project. S.E.D., M.S., and C.R. obtained funding for the project, and conceived the study. S.E.D. also conducted experiments, analyzed data, and contributed to the writing of the manuscript. All authors reviewed the manuscript.

Abstract

Inhalation of cigarette smoke (CS) is a risk factor for multiple sclerosis (MS) and it is estimated to account for 20% of disease cases. However, the mechanism of how CS exposure promotes autoimmunity in MS is not understood. To investigate the potential mechanisms driving this immune phenotype, we investigated the effect of CS exposure on the development of myelin-specific autoimmunity in experimental autoimmune encephalomyelitis (EAE) models of MS. We observed that CS exposure enhanced myelin-specific Th1 responses in peripheral lymphoid compartment, but puzzlingly delayed the onset of EAE. Further studies done using a Th17 passive EAE model revealed that EAE was delayed with CS because myelin-specific T cells were retained in the lungs where they became hyperactivated and produced greater levels of Th1/Th17 cytokines and GM-CSF. Neutralizing IL-12p40 reduced these effects of CS on T cells. This work identifies a potential mechanism for how CS exposure enhances MS and identifies a potential target for treatment.

Key words: multiple sclerosis; experimental autoimmune encephalomyelitis; cigarette smoking; lungs; T cells; Th1 cells; IL12-p40; autoimmunity

Introduction

More than a billion people in the world currently smoke (1). This habit has a detrimental effect on lung and whole body health and is a major cause of preventable death worldwide (1). Though tobacco consumption has undergone a decline in recent decades (2), consumption rose during the 20th century (3), coinciding with the rising prevalence of autoimmune diseases (4, 5). Epidemiology studies have provided evidence that inhalation of CS increases the risk for a number of autoimmune diseases including MS, rheumatoid arthritis (RA), systemic lupus erythematosus (SLE), Crohn's disease, and psoriasis (6). Studies that examined the impact of active and passive smoke exposure on RA or MS risk estimated that a third of RA cases (7), and 20% of MS cases (8) are preventable if people stopped smoking (7). For MS, smoking increases disease risk in a dose-dependent manner with a more prominent effect apparent in males (odds-ratio, OR=1.8) compared to females (OR=1.4) (9) and this effect is sustained even after 5 years after quitting smoking (9, 10). Despite the male bias in the effect of CS on MS risk, tobacco consumption increased more substantially in women during the middle of the 20th century, correlating with the rise of MS in females during this period (11).

Beyond disease risk, there is evidence that smoking tobacco hastens disability accrual in people with established MS (6, 12, 13). Each year of smoking post-MS diagnosis is associated with 5% accelerated time to conversion to secondary progressive MS (SPMS), a stage of disease where patients show a slow and steady accumulation of disability (13). The number of new brain lesions and brain lesion volumes are also greater in the white matter (WM) of MS patients who smoke as assessed by magnetic resonance imaging (12, 14, 15); this suggests that cigarette smoking increases immune-mediated damage in the CNS. In contrast, quitting cigarette smoking is associated with a slowed onset of SPMS and a delay in reaching certain disability milestones such as needing a cane to ambulate (13, 16), making this behavioral intervention as powerful as any available disease modifying therapy in slowing MS progression for those who smoke. Despite this knowledge, the mechanisms by which cigarette smoking enhances MS is unknown.

Clues to potential mechanisms have been provided by epidemiology studies that compared the effect of cigarette smoking versus oral consumption of tobacco on MS risk. It was found that, unlike smoking tobacco, consumption of Swedish snuff, a tobacco product that is absorbed through the oral mucosa, protects against MS (9). Furthermore, switching from cigarettes to snuff was demonstrated to slow the rate of disease progression (13). These findings, coupled with studies that showed that occupational exposure to organic solvents can increase MS risk (17), gave rise to the idea that the lung irritation associated with the inhalation of smoke particles drives MS (9). Beyond this, epidemiology studies have found that exposure to CS positively interacts with major histocompatibility complex II (MHC-II) risk alleles to increase MS and RA risk (18-20). In the case of MS, smokers who carry the major MHC-II risk allele HLA-DRB1*1501 and are deficient in a protective MHC class I allele have 13.5-fold greater risk of MS compared to those who do not smoke or carry these risk alleles (21), suggesting that CS promotes Th cell autoimmune mechanisms. Consistent with this, in SLE and RA, smoking has been shown to also promote autoantibody generation, a process that requires T cell help (22-24). In RA, CS also promotes citrullination of proteins in the lung, which is associated with an increased generation of anti-citrullinated protein antibodies and a worse disease prognosis (24). While there is evidence of increased protein citrullination in the brains of MS patients, there is no evidence of increased T cell reactivity against citrullinated versions of these CNS antigens (25). Taken together, the literature indicates that lung irritation caused by cigarette smoking enhances T helper cell responses in MS, although the mechanisms remain unknown.

To gain insights into the effects of CS exposure on MS-related autoimmunity, we employed EAE and a whole-body passive CS exposure system in order to study potential mechanisms underlying these effects. We found that CS exposure promoted IFN-γ production by myelin-specific Th1 cells that were detected in the peripheral lymphoid organs, but unexpectedly delayed the onset of EAE. Further studies in a passive transfer model of EAE where IL-23 polarized, congenically-labelled myelin-reactive Th17 cells were transferred into CS- or ambient air (AA)-exposed hosts demonstrated that smoking created a pro-inflammatory environment in the lung that

promoted the activation and IL-17 and GM-CSF expression by the transferred myelin-reactive Th cells. This effect on the myelin-reactive T cells was retained even after these cells invaded the CNS. Despite exhibiting greater pro-encephalitogenic activities, transferred myelin-reactive Th cells did not enhance passive or active EAE in CS hosts since the lung inflammation detained some of these cells in the lung. In contrast, when myelin oligodendrocyte glycoprotein (MOG) T cell receptor transgenic mice were exposed to CS, this factor promoted mild neuroimmunity. All of these effects of CS on myelin-specific Th autoimmunity were mainly observed in males, which associated with a greater upregulation of IL-12p40 and greater overall inflammation in the lung. Neutralizing IL-12p40 activity negated these effects of CS on myelin-reactive Th cells both *in vivo* and *in vitro*. These studies raise the prospect of using inhaled anti-IL-12p40 as an add-on therapy to treat lung inflammation in MS patients who smoke.

Methods

Mice

Male and female C57BL6/J mice (Stock#664), female CD45.1 congenic mice on the C57BL6/J background (PepBoy; B6.SJL-Ptprca Pepcb/BoyJ; Stock# 002014), male and female 2D2 T cell receptor transgenic mice (2D2 mice; C57BL/6-Tg(Tcra2D2,Tcrb2D2)1Kuch/J; Stock#6912) were all from the Jackson Laboratory. The latter mice were bred in house in pairings of heterozygote males with wild-type C57BL/6J females. 2D2 heterozygote offspring were genotyped using flow cytometry of PBMCs after staining for CD4 and T cell receptor (TCR) Vβ11 chain as described previously (26). All mice were housed within a specific pathogen-free facility at the University Health Network (UHN) and experiments were performed under an animal use protocol (AUP 5937) that was approved by the UHN animal care committee.

Exposures to CS and Ambient Air (AA) and Cotinine Measurements

Adolescent mice were exposed to CS using a whole-body exposure system (SIU48; Promech Lab Inc., Vintrie, Sweden) as described previously (27). This exposure system was housed in a chemical fume hood and combusted research grade cigarettes with

filters removed (Tobacco and Health Research Institute, University of Kentucky, Lexington, KY). Generated CS was puffed into a central chamber where freely moving mice were housed in compartments with their cage mates with food and water removed. Exposures were initiated when mice were 7 weeks of age and consisted of twice daily 50 min sessions (separated by 3 h) where they were housed in the smoke chamber and exposed to CS from 12 serially burned cigarettes. Exposures were conducted for 5 days a week for 8-10 weeks and were preceded by an initial 3 day acclimatization period where mice were placed in the exposure box for increasing lengths of time. This CS exposure regimen was well tolerated and produced total particulate matter in the exposure chamber ranging from 600 to 700 µg/L. AA-exposed controls were brought into the same room and at the time of CS exposures were placed into an empty cage having similar dimensions as the cage used in the exposure system with water and food removed. To estimate the dose of acute CS exposures, blood was drawn within 30 min of CS- or AA- exposures and was centrifuged (5000 rpm x 5 min) to collect serum. Cotinine was measured in 1:3 diluted serum using an ELISA kit (Origene).

Lung Pathology

Mice were anaesthetized with isoflurane and perfused with 1 x PBS containing 5 U/mL of heparin. The chest was opened and surgically dissected to reveal the lungs and trachea. The trachea and esophagus were cut below the jaw and the lung and connected heart were dissected out of the chest cavity and placed on wax weigh paper. A cannula was inserted into the trachea (VWR 427411, 0.5 cm) and was tied in place by affixing surgical twine. To prepare formalin-fixed paraffin sections, lungs were first inflated with formalin. For this, a 50 mL syringe was filled with neutral buffered formalin and this was gravity fed through surgical tubing to a 23G needle that was placed in the canula. After the lungs were fully inflated, the trachea was tied off below the level of the cannula and the heart-lung was stored in 10% formalin. After 3-7 days, the lungs were grossed, processed and embedded in paraffin with the right lung embedded longitudinally, and the left lung upper, middle, and lower lobes embedded in cross-section. Hematoxylin and eosin (H&E) staining and CD45 immunohistochemistry (IHC) (anti-CD45 antibody raised in rat, clone 30F-11, BD) were conducted as previously described using our established protocols (28).

Dual CD3 and B220 IHC was conducted via similar method with the following modifications. After de-waxing, antigen retrieval, peroxidase quenching, and blocking (28), sections were stained overnight at 4°C using a polyclonal anti-human CD3 antibody raised in rabbit (1:1000, Dako). The following day, sections were washed 3 x in PBST and this was followed by probing with secondary antibody (HRP conjugated, goat, anti-rabbit antibody, clone BA-1000, Vector) and incubation with HRP-streptavidin complexes (universal ABC-HRP kit, Vector labs) (28). After a final washes, immune complexes were developed using DAB (Vector SK4100) (28). Sections were then re-blocked in the following blocking buffer (2% BSA in 2% rabbit serum) that contained Avidin (Avidin Biotin kit, Vector labs) and then incubated overnight at 4°C with anti-B220 antibody (1:500, clone RA3-6B2, BD Biosciences) in blocking buffer that contained biotin. Slides were washed with PBST and then incubated with biotinylated rabbit anti-rat secondary antibody (1:200, Vector labs) for 30 min at RT. After an additional wash, sections were incubated for 30 min at RT with Avidin-Alkaline Phosphatase (1:1000; BioShop) in 1 x PBS. Slides were washed again with BST, and antibody-AP complexes were developed using Vector blue as a chromogen (Vector labs). Slides were then dehydrated and then cleared with Citrosolve and cover-slipped using Permount (both from Fisher).

For CD45.1 immunohistochemistry, the lungs and heart with attached trachea were harvested and canulated as described above except that the lungs were inflated with 500 µL of a 2:3 solution of 1 x PBS: optimal cutting temperature (OCT) compound using a 23 G needle and syringe. The inflated lungs were tied off below the cannula and submerged in the PBS: OCT solution until all specimens were collected. After grossing the lungs, they were embedded in OCT in melting 2-methyl butane cooled by liquid nitrogen. OCT embedded lungs were cut at 4 µm and stained using a CD45.1 antibody (1:1000, clone A20, Biolegend) and the mouse on mouse (M.O.M) kit (Vector laboratories) according to kit directions. In brief, prior to incubation with primary and secondary antibodies, sections were air-dried for 10 minutes and then were fixed in ice-cold methanol for 15 min. Slides were washed in 0.5% PBST (3 x 5 min) and endogenous peroxidases were blocked with 3% hydrogen peroxide in methanol. Sections were blocked using the blocking solution provided in the M.O.M. kit for 30 min

at RT then washed with PBST. After secondary antibody detection, sections were incubated with streptavidin-HRP (universal ABC HRP kit, Vector labs) and then sections were developed with DAB, counterstained with hematoxylin, dehydrated, cleared with Xylene, and were mounted with Permount according to our published protocol for M.O.M. IHC (28).

Lung Digestion and Flow Cytometry to Examine Lung Mononuclear Cell Composition

The lungs were dissected as above and placed in a conical tube containing ice-cold RPMI 1640 (Life Technologies) and 2% fetal bovine serum (FBS; Wisent). Lung lobes were transferred to a petri dish containing 5 mL of ice-cold RPMI and were scissor minced and transferred to a 50 mL conical tube. Five mL of 2 x digestion buffer containing 300 U/mL type 1 collagenase (Worthington) and 10 U/mL DNAse I (Sigma) in RPMI 1640 were added to the tube and the tissue was agitated for 1 h on a 37°C shaker. The cells were then dissociated through a 70 micron sieve and transferred into 15 mL conical tube. The cells were centrifuged at 300 x g for 10 min at 4°C. The supernatant was discarded and red blood cells were lysed with ACK buffer (0.15 M NH_4Cl, 10 mM $KHCO_3$, 0.1 mM Na_2EDTA) for 1 min and 15 s (26), and the lysis stopped with RPMI. Cells were centrifuged again, counted and washed with FACs buffer. Cells were incubated with Fc Block (5 µg/mL; BioLegend) for 15 min at 4°C and then washed in FACS buffer. Cells were incubated with the antibody cocktail detailed in Suppl. Table 1 ("Lung Immune Cells Panel 1") and Fixable Viability Dye eFluor 506 (1:1000; Invitrogen) in the dark for 30 min at 4°C and were washed again. Cells were analyzed and unmixed using a Sony SP6800 Spectral cell cytometer and software and data were analyzed in FlowJo (version 10). Cell populations were gated using fluorescent minus one (FMO) controls.

MOG p35-55/CFA Immunization and Active EAE Induction

Mice were immunized subcutaneously at two sites of the chest (50 µl/side) with an emulsion containing 100 µg MOG p35-55 (Genemed Synthesis) and Complete Freund's Adjuvant containing 200 µg of heat-killed *Mycobacterium tuberculosis* (H37RA, Difco Laboratories) (26). For active EAE induction, mice were also injected with 100-250 ng (lot-dependent) *Bordetella pertussis* toxin (PTX, #181, List Biologicals) on days 0 and 2

following immunization. Mice were examined daily for clinical signs of EAE using a five-point scale: (0) no clinical signs; (1) limp tail; (2) hindlimb or foot weakness; (3) complete hindlimb paralysis in one or both hindlimbs; (4) hindlimb paralysis plus some forelimb weakness; (5) moribund or dead. Mice that died from EAE were assigned a score of five for the remainder of the experiment. Cumulative score was calculated for each mouse by adding up the daily scores over the period of observation (26). Mice were checked for the hindlimb clasping reflex by elevating them by the tail and making note if the hindlimbs curled inwards (clasping) or remained splayed (29).

Measuring MOG p35-55 Reactive T cell Recall Assays in Spleen and Draining Lymph Nodes

The effects of CS exposure on Th cell priming were assessed as follows. Mice were immunized with MOG p35-55/CFA and at nine days post-immunization, the recall proliferative and cytokine response of the spleen and draining lymph nodes to MOG p35-55 were examined. For these studies, the draining lymph nodes and spleens were isolated from mice and dissociated into a single cell suspension. Cells were washed, centrifuged (300 x g, 10 min), and red blood cells were lysed with ACK lysis buffer (26). The lysis was stopped via the addition of excess 1 x PBS. After a second centrifugation, cells were resuspended in Complete RPMI media ([CM] RPMI 1640, 2 mM L-glutamine, 1 mM sodium pyruvate, 0.1 mM nonessential amino acids, 100 U/mL of penicillin, 0.1 mg/ml of streptomycin (all from Life Technologies), 50 µM 2-mercaptoethanol (BioShop), and 10% fetal bovine serum (FBS; Wisent)), and were counted using a hemacytometer. Cells were plated in 96-well flat-bottomed plates ($0.5x10^6$ cells/well) together with 0, 2, 5, and 10 µg/ml MOG p35-55. Cytokines were measured in culture supernatants at the time of peak production (IFN-γ at 48 h, IL-17A at 72 h) using Ready-Set-Go ELISA kits (ThermoFisher) or the LegendPlex T helper cytokine panel (Biolegend). In addition, the number of MOG p35-55 $CD4^+$ T cells that had expanded after immunization was estimated in the spleen by examining the number of splenocyte $CD4^+$ T cells that divided as assessed by CFSE dilution assay (Molecular Probes) after re-stimulation *ex vivo* with MOG p35-55 antigen. For this assay, $10x10^6$ spleen cells were labelled with 0.5 µM CFSE according to instructions provided in the kit. Cells were then plated in duplicate in 24 well plates (2.5×10^6 cells/well) together with MOG p35-55

(5 µg/mL) for 72 h in a 37°C incubator with 5% CO_2. Cells were then harvested, washed with 1 x FACS buffer, and stained with LIVE/DEAD™ Fixable Aqua Dead Cell Stain (1:1000; Invitrogen) and the antibody cocktail detailed in Suppl. Table 1 ("T Cell proliferation Panel"). The number of MOG p35-55 reactive Th cells was estimated as the frequency of $CD44^{hi}$ $CD4^{+}$ T cells that specifically divided in response to MOG p35-55 multiplied by the total amount of live splenocytes that were counted at the hemacytometer.

Passive transfer EAE

For passive transfer EAE, 8-week-old female C57BL6/J mice or CD45.1 Pepboy mice were immunized with MOG p35-55/CFA as described above. At day 9 post-immunization, the draining lymph nodes and spleens were harvested and mononuclear cells isolated and re-suspended in CM as described above. Cells were plated at 8 x 10^6/ml in 75 cm^2 vented tissue culture flasks with 10 µg/ml of MOG p35-55 for 3 days in the presence of 10 ng/mL IL-23 (R&D Systems). After 3 days of culture, cells were washed three times in 1 x PBS and then 10-20 x 10^6 cells (experiment-dependent) were injected into recipient male or female CD45.2 C57BL6/J mice that had been exposed to AA or CS for 8-10 weeks previous. Exposures to CS and AA were continued throughout the experiment and mice were checked for development of clinical signs.

Histological Scoring of EAE

Brains and spinal cords from mice with active EAE were isolated, preserved in 10% neutral buffered formalin (Sigma) for 7 days, processed in paraffin, and embedded in a single paraffin block (10–12 spinal cord and 6 brain sections/block) according to our published protocol (30). Cross-sections (5 µm) were cut (Center for Phenogenomics, Toronto, ON) and stained with Luxol Fast Blue (LFB) to visualize myelin and percent demyelination was scored as described previously (30). IHC for mouse CD45 was performed as previously described in (30). Sections were then dehydrated in successive ethanol baths, cleared in xylene, and mounted with Permount. The scoring of $CD45^{+}$ leukocytes/mm^2 in white matter was conducted using ImageJ using our published protocol (30).

CNS Mononuclear Cell Isolation

CNS mononuclear cell isolation was conducted as described previously (31). In brief, mice were anaesthetized with isoflurane and transcardially perfused with 20 mL of 1 x PBS containing 5 U/mL of heparin. Spinal cords and brains were dissected from mice and then placed in 1 x HBSS containing 10% FBS on ice. For each mouse, the spinal cord was extruded from the spinal column using 1 x HBSS contained in a 23G needle and 3 mL syringe. CNS tissue pieces were washed in 1 x HBSS, centrifuged (750 x g at 4°C for 10 min), resuspended in 1.25 mL of HBSS, and were scissor minced. Then an equal volume of 1 x HBSS containing 600 U/mL of type IV collagenase (Sigma) and 10 U/mL of DNAse I (Sigma) was added to minced tissue and this was incubated at 37°C for 45 minutes in an incubator. Digested tissue was dissociated through a 70 micron sieve into fresh 1 x HBSS. Cells were collected and centrifuged at 750 x g at 4°C for 10 minutes and the cell pellet was resuspended in 40% Percoll and carefully layered onto 70% Percoll (in 1 x HBSS). After a centrifugation (500 x g at RT for 20 min with no brake), cells were collected from the interface and then resuspended in ice-hold 1 x HBSS. Cells were centrifuged again (300 x g for 10 min at 4°C) and then were resuspended in complete RPMI for counting.

Flow Cytometry Characterization of Intracellular Cytokine Expression and Activation Markers by MOG p35-55 reactive Th cells during Passive EAE studies

For measurement of cytokines, isolated CNS and lung mononuclear cells CM were incubated in the absence and presence of 20 µg/ml MOG p35-55 overnight (12 h) in a 37ºC incubator with 5% CO_2. GolgiStop (BD Biosciences) was added in the last 6 h of culture. Cells were washed with 1 x FACS buffer, incubated with Fc Block (5 µg/ml; BioLegend) for 15 min at 4°C and then washed in FACS buffer. Cells were then incubated with antibody cocktails detailed in Suppl. Table 1 ("Cytokine Production in CD45.1 AT-EAE" panel for experiments where passive EAE was induced by transferring $CD45.1^+$ cells, and "Cytokine Production in AT-EAE" panels 1 and 2 when C57BL/6J donors were used for passive EAE) and LIVE/DEAD™ Fixable Aqua Dead Cell Stain (1:1000; Invitrogen) in the dark for 30 min at 4°C, and were washed again. Cells were fixed with 4% paraformaldehyde in 1 x PBS for 10 min at 4°C, washed, and then incubated with 1 x Perm Wash buffer (BD Biosciences) in the dark for 30 min at 4°C.

After washing cells 3 x with Perm Wash buffer, cells were incubated with the intracellular antibody cocktails detailed in Suppl. Table 1 ("Cytokine Production in CD45.1 passive transfer-EAE". or "Cytokine Production in passive transfer-EAE" panels 1 and 2 when C57BL/6J donors were used for passive EAE). In all cases, cells were incubated in the dark with antibodies diluted in FACS buffer 30 min at 4°C and washed again 1x Perm Wash. Cells were analyzed using a Fortessa X-20 or a Cytoflex-LX cytometer and data analyzed in FlowJo (version 10). Cell populations were gated using FMO controls.

To assess the activation status of T cells or the maturation status of DC in the lung, cells were processed and washed and viability dye and cell surface staining was performed using the antibody cocktails detailed in Suppl. Table 1 ("Activation of T cells" panel for experiments where passive EAE was induced by transferring CD45.1^{+} cells, and "Activation of 2D2 T cells" panel for 2D2 mice and "DC maturation status in the Lung"). Cells were analyzed using a Cytoflex-LX cytometer and FlowJo software.

Quantification of Cytokines and Chemokines in Lung Homogenates

Lungs were isolated from mice that had been exposed to CS or AA for 8 weeks and immunized 9 days previous with MOG p35-55/CFA and were snap-frozen in liquid nitrogen and stored at -80°C. Lungs were weighed and then homogenized in T-PER buffer according to instructions (Thermo Scientific). Homogenates were incubated on ice for 1 h and then centrifuged for 10 min at 10,000 x g at 4°C. Supernatants were aliquoted and frozen at -80°C. Protein levels in the lysates were measured using a BCA Assay (Pierce). Cytokine and chemokine levels were measured in supernatants by Eve Technologies using the Mouse Cytokine/Chemokine 32-Plex Discovery Assay Array (MD32) panel. The following additional analytes were measured using the following ELISA kits: amphiregulin (RayBiotech), BAFF and CXCL13 (R&D Systems), IL-23 ELISA Max kit and IL-33 LegendMax ELISA kit (Biolegend), and Verikine-HS Mouse IFN-α all subtype ELISA kit (PBL Biosciences). All cytokine levels were expressed per mg of protein.

Dendritic Cell (DC): T Cell Co-culture Assays

Mononuclear cells were isolated from pooled lungs of AA- and CS-exposed male C57BL/6J mice (n=5/group) as described above, and DCs were enriched from this preparation using the mouse Pan Dendritic Cell Isolation Kit (Miltenyi). Isolated DCs ($2.5x10^4$) were resuspended in CM and plated in triplicate in round-bottom plates with 0 or 6 ng/mL LPS and 0-20 µg/mL MOG p35-55 for 6 h at 37°C and 5% CO_2. Meanwhile, $CD4^+$ T cells were enriched from spleens of 3 2D2 male mice using the MojoSort Mouse CD4 T Cell Isolation Kit (Biolegend). A portion of these cells were stained with Cell Proliferation Dye eFluor450 according to the product directions (eBioscience). 2D2 $CD4^+$ T cells (5.0×10^4) were placed on top of DCs in the round-bottomed plates cells and were cultured for 2-3 days at 37°C and 5% CO_2. Cells were then washed with FACs buffer, and surface FACS staining was performed to assess dye dilution in the $CD44^{hi}$ 2D2 $CD4^+$ T cells as described above, using the antibody cocktail detailed in Suppl. Table 1 ("DC:T cell Co-culture" panel 1). For cytokine assessment, cells were re-stimulated with 50 ng/mL PMA and 500 ng/mL Ionomycin for 4 h, with GolgiStop added in the last 2 h of culture and cells were then stained for surface and intracellular FACS as described above, using the antibody cocktails detailed in Suppl. Table 1 ("DC:T cell Co-culture" panel 2). Cells were analyzed using a Cytoflex-LX cytometer and data analyzed using FlowJo.

To assess the role of IL-12p40 signalling in T cell priming by lung DCs, a similar co-culture experiment was performed, with the addition of either 10 µg/mL of anti-mouse IL-12p40 neutralizing antibody (clone C17.8, BioLegend) or isotype control antibody (clone RTK2758, BioLegend) to the cultures starting during the pre-activation phase when DCs were incubated with LPS and MOG p35-55. After the co-culture of DCs and 2D2 $CD4^+$ T cells for 2-3 days at 37°C and 5% CO_2, cells were stained as described above using "DC:T cell Co-culture" panels 1 and 2. Cells were analyzed using a Cytoflex-LX cytometer and data analyzed as described above.

IL-12p40 Blockade in Lung

Initially we tested the effect of IL-12p40 antibody (clone 2A3; BioXCell) in neutralizing IL-12p40 levels in the lungs of naive mice, which have detectable levels of IL-12p40 expression at steady-state. This was done by administering 50, 125, or 200 µg/mouse

of the InVivoMab anti-mouse IL-12p40 antibody (clone C17.8; BioxCell) to mice (n=2/group) intranasally or intratracheally, and then euthanizing mice 3 days after for measurement of IL-12p40 in lung, spleen, and small intestine homogenates using an anti-IL-12p40 ELISA kit (Biolegend). This study demonstrated that 125 µg intranasal administration of the antibody specifically lessened IL-12p40 levels in the lung, while higher doses or intratracheal administration led to systemic depletion of the cytokine (Supplementary Fig. 1).

AA or CS-exposed male recipients were induced to have EAE with pre-primed female MOG p35-55 reactive CD45.1^{+} cells. Two days prior to and 1 day after the adoptive transfer of the myelin-reactive cells, the recipient C57BL/6J mice were anaesthetized with isoflurane and were administered 125 µg/mouse of IL-12p40 antibody or InVivoMAb rat IgG2a isotype control (clone 2A3; BioXCell) intranasally. Mice were euthanized on day 4 post-transfer, and lungs were collected for flow cytometry as described above, using antibody cocktails detailed in Suppl. Table 1 ("*In Vivo* IL-12p40 Blockade" panel). Data were analyzed using a Cytoflex-LX cytometer and FlowJo software.

Statistical Analysis

Data were analyzed with GraphPad Prism (v10). Data are showed as mean ± SEM. For studies that contained more than 2 groups, data were analyzed using a 2-way ANOVA followed by a Bonferroni post-hoc test. For experiments that only used males and compared AA and CS, two-tailed Mann-Whitney U test was used. P values of $p \leq 0.05$ were considered statistically significant.

Results

Exposure to CS Induces Lung Immune Cell Infiltration and the Formation of Immune Micro-clusters Around the Lung Bronchioles and Blood Vessels

To study the mechanisms linking CS exposure to promotion of myelin-specific autoimmunity, we employed a whole-body CS exposure system that delivered puffs of CS to freely moving mice housed in a chamber (32). Mice were exposed to CS in 2 x 50

min sessions per day, 5 days/week for a total of 8 weeks, while controls exposed to AA were placed in a cage with similar dimensions as the exposure chamber at the same time of CS-exposures. Consistent with past studies using this regimen, each bout of CS acutely raised cotinine in serum to levels that are similar to that reported for heavy smoking humans (Fig. 1A) (32, 33). When this CS exposure regimen was administered to male mice over 8 weeks, it triggered the increased infiltration of leukocytes in the lung as detected using CD45 immunohistochemistry (Fig. 1B-E). Leukocytes were not only more numerous with CS, but were sometimes organized in micro-clusters surrounding the bronchioles or blood vessels (Fig. 1E). Quantification of CD45 staining revealed that the average size of each individual cluster (Fig. 1C) as well as the area occupied by these clusters (Fig. 2D) in CS-exposed mice were increased relative to the levels seen in AA-exposed controls.

To gain further insights on how the lung immune composition changed with CS exposure, in separate studies, we quantified different immune subsets in digested lungs taken from CS- and AA-exposed male and female mice using flow cytometry (gating strategy shown in Fig. 2F). This analysis confirmed an increase in $CD45^+$ leukocytes with CS-exposure in the lungs of males, with a similar trend evident in lungs of females (Fig. 2G). Similar to our past studies using this CS exposure regimen (27), we observed greater levels of non-resident macrophage populations and classical dendritic cells in lungs of male and female mice with CS- versus AA-exposure (Fig. 2H). In addition, we detected a significant increase in B and T cells in the lungs of males with CS (Fig. 2H).

Since T and B cells were the cell populations that underwent the greatest increase in the lungs with CS exposure, we immunolocalized these cells in lung sections of male CS- and AA- exposed mice. These studies revealed that B cells were rare, whereas T cells scattered sparsely throughout the lung parenchyma in lungs of the AA-exposed mice (Supplementary Fig. 2A). By contrast, in males exposed to CS, T cells were organized in larger micro-clusters, which sometimes also contained B cells (Supplementary Fig. 2B-D). These findings suggest the beginnings of tertiary lymphoid structure (TLS) formation in the lung after 8 weeks of CS exposure. Thus, CS induced lung inflammation that was exacerbated in males.

Exposure to CS Enhances Myelin-Specific Th1 Responses in the Peripheral Lymphoid Organs of Mice During EAE

We next assessed whether prolonged CS exposure in mice could promote myelin-specific Th1 or Th17 responses during EAE, a common immune-based model of MS. To this end, male mice were exposed to CS or AA for 8 weeks using the same regimen and then were immunized with MOG_{35-55}/CFA. The spleen and draining lymph nodes were then collected from mice at day 9 post-immunization and recall T cell cytokine and proliferative response to MOG p35-55 antigen were assessed by ELISA and CFSE-dilution assay, respectively. We found that CS enhanced IFN-γ secretion by MOG p35-55-reactive Th cells in the spleen and in the draining lymph nodes (Fig. 2A-B); TNF and IL-13 production by MOG p35-55-reactive T cells was also greater in the lymph nodes of males with CS exposure, whereas IL-17, IL-4, and IL-10 were not significantly altered (Fig. 2A-B). These increases in MOG p35-55-Th1 cytokine production were not due to greater abundance of MOG p35-55-responding $CD4^+$ T cells (Fig. 2C-E). A similar trend for greater MOG p35-55-specific Th1 cytokine production in spleen, but not lymph node cells was seen in CS-exposed females; however, in this case IL-13 was decreased with CS-exposure (Supplementary Fig. 3A-B). Thus, CS exposure enhanced myelin-specific Th1 immunity, especially in male mice.

Prophylactic Exposure to CS Attenuates EAE Selectively in Male Mice

Given these effects of CS exposure in promoting myelin-specific Th1 immunity, we initially had hypothesized that mice exposed to CS would develop a more severe course of EAE compared to AA-exposed controls. To address this, male and female mice were exposed to CS or AA for 8 weeks, were immunized with MOG p35-55/CFA and provided pertussis toxin, and then monitored for clinical signs. Exposures to CS or AA were continued throughout the clinical monitoring period (Fig. 3A). Contrary to our expectations, but consistent with past reports of CS exposure on EAE in female C57BL6/J mice (34, 35), MOG p35-55-induced EAE was attenuated with CS-exposure in males, with these mice exhibiting a delayed disease, decrease in peak score, and cumulative score compared to AA-exposed controls (Fig. 3B-E). Pathological analysis of the spinal cord at end-point confirmed reduced histological EAE with decreased

leukocyte infiltration and percentage demyelination in the males exposed to CS (Fig. 3F-H). In contrast, females CS-exposed mice did not differ from AA-exposed controls for any of these measures (Fig. 3B-G). Thus, despite exhibiting worse lung inflammation and myelin-specific Th1 autoimmunity, male mice paradoxically developed less severe EAE.

Nicotine, the addictive chemical component of tobacco, is known to have anti-inflammatory properties in EAE (36) and MS (9) and is speculated to account for the protective effects of CS exposures on EAE. Since nicotine and its biproduct cotinine are eliminated from the blood within hours of CS-exposure (27) we addressed whether stopping CS exposures at 5 days prior to the onset of EAE would negate this protective effect of CS on EAE in male mice (Fig. 3I). Despite smoking cessation, mice exposed to CS still developed milder clinical signs and a slight delay in EAE as compared to AA-exposed controls (Fig. 3J-K), indicating that another factor was involved in mediating these protective effects of CS.

CS Attracts Myelin-Specific Th Cells to the Lung Where They Acquire Increased Pro-Inflammatory Characteristics

The discordance between the effect of CS exposure on myelin-specific Th1 responses and EAE suggested that the MOG p35-55-reactive T cells were efficiently primed in the draining lymph nodes of mice, but failed to traffic to the CNS. Past studies that used a passive T cell transfer model of EAE in rats demonstrated that after injection, myelin-reactive Th cells traffic through the blood to the lung and bronchiole-associated lymphoid (BALT) structures, where they reside for several days, prior to re-entering the blood stream (and spleen) to travel to the CNS (37). This study showed that this passage through the BALT conveyed migratory capacity to the myelin-reactive Th cells (37). To investigate whether the MOG p35-55-reactive T cells were being increasingly retained in the lung with CS-exposure, we employed a passive transfer model of EAE where MOG p35-55-reactive Th cells derived from immunized CD45.1 congenic female PepBoy mice were expanded with IL-23 and MOG p35-55 and then transferred into CS- or AA-exposed hosts. IL-23 was included in the donor cultures to enhance the encephalitogenic capacity of the MOG p35-55-reactive Th cells to overcome the

resistance of C57BL6/J mice to passive EAE. Similar to our findings in the active EAE model, CS-exposed males developed passive EAE with a delayed onset compared AA-exposed controls; however, eventually CS-exposed mice attained equivalent clinical scores as the AA-exposed controls (Fig. 4A-B). When this same study was conducted in females only a small delay in EAE was seen with CS exposures (Supplementary Fig. 3C).

To investigate the phenotype of transferred MOG p35-55-reactive $CD4^+$ T cells that infiltrated the CNS, mononuclear cells were isolated from digested spinal cord and cerebellum tissue at a time when clinical scores were equivalent between CS and AA-exposed male mice (*grey arrow,* Figure 4A) and flow cytometry was used to enumerate the total number of cells and the CD45.1 transferred MOG p35-55-reactive Th effector cells (see gating strategy in Fig. 4C). Despite having the same number of total (host plus donor) leukocytes in the CNS (Fig. 4D), the CS-exposed mice had only half the amount of $CD45.1^+CD4^+$ cells as AA-exposed controls (Fig. 4E). However, the percentage of $CD45.1^+CD4^+$ that had IL-17 or co-produced IL-17 and GM-CSF was doubled (Fig. 4F). GM-CSF is a cytokine that is expressed by pathogenic Th1 and Th17 cells that is absolutely required for initiating the CNS inflammatory response required for EAE development (38). We detected that for each CD45.1 Th17 effector cell that made it to the CNS of CS-exposed hosts, there were twice as many leukocytes recruited (Fig. 5G), consistent with the idea that the individual T cells were more highly encephalitogenic. Thus, CS in the hosts made the transferred MOG p35-55-reactive cells upregulate GM-CSF, but also delayed their entry to the CNS.

To see whether the transferred MOG p35-55-reactive Th cells were being retained in the lung with CS, we repeated passive transfer EAE experiments, but harvested cells from mice at a time when clinical signs had presented in the AA group but were delayed in the CS group (*black arrow*, in Fig. 4A). These experiments revealed a 5-10-fold higher number of $MOG_{35\text{-}55}$-specific IL-17^+ and IL-17^+IFN-γ^+ $CD4^+$ T cells in lungs of CS compared AA-exposed mice (Fig. 4H, see representative gating in 4I). We also detected an overall increase in host IFN-γ^+CD4^+ T cells in the lung (those that showed responses in the absence of MOG p35-55), consistent with the idea that the inflamed environment in the lung promotes IFN-γ production by $CD4^+$ T cells (Fig. 4H-I). Our findings are

therefore consistent with past findings describing increased IFN-γ and IL-17 by lung $CD4^+$ T cells of CS-exposed mice in response to polyclonal stimulation (39, 40). In contrast to findings in the lung, CS exposure did not alter the total numbers of MOG p35-55-specific $CD4^+$ cells in the spleen (Fig. 4J).

In light of past studies that showed that T cells become activated in the BAL of mice exposed to CS and in human smokers (27, 41), we conducted further passive EAE studies in CS- and AA-exposed mice and investigated expression of activation markers as well as GM-CSF of the MOG p35-55-specific (IL-17A^+) $CD4^+$ T cells in the lung. These studies revealed that the transferred MOG p35-55-specific T cells expressed significantly higher levels of IL-17 and GM-CSF (as assessed by MFI) (Fig. 4K) as well as activation markers CD25, PD-1, CD69 (Fig. 4L). When similar studies were done in CS females, no upregulation of pro-inflammatory cytokine production or activation marker expression was evident in the CD45.1 T cells, with the exception of CD69, which was higher with CS, but is also a marker of tissue-residency. This suggested that the transferred T cells did not reach a similar activation state in the lungs of females (Supplementary Fig. 3D-G). We detected no change in activation markers on CD45.2 $CD4^+$ T cells, suggesting that only the T effector cells could achieve a higher state of activation in the CS lung (Supplementary Fig 3H-I). Finally, to investigate whether the transferred myelin-reactive CD45.1 cells were located within TLS-like structures, we reserved a few lungs from the experiment done in males and conducted IHC staining for CD45.1. We observed $CD45.1^+$ cells scattered through the lung parenchyma, but also within the para-bronchiole immune clusters (Fig. 4M). Thus, CS-exposure caused retention of transferred MOG p35-55-reactive Th17 effector cells in the lungs of male mice where these cells became increasingly activated and upregulated expression of GM-CSF.

CS Exposure in the Lung Amplifies Cytokine Production but Does Not Provide an Antigen Signal for Naive MOG p35-55-Reactive T Cells

The finding of upregulated activation marker expression by the transferred MOG p35-55-specific T effector cells in the lung with CS exposures raised the prospect that the CS particles may be providing an antigenic stimulus for these T cells in the lung. To

address this, we conducted studies where we exposed healthy naive 2D2 MOG-specific T cell receptor transgenic mice to CS or AA. In this model, no external source of MOG p35-55 or adjuvant was provided to mice and 2D2 $CD4^+$ T cells become educated in response to interactions with gut commensals or pathogens at mucosal surfaces (42). As was the case in the passive transfer EAE model, CS induced a greater accumulation of leukocytes and 2D2 $CD4^+$ T cells in the lung (Fig. 5A-B), however, the majority of these T cells were naive and this proportion did not change with CS (Fig. 5C). Furthermore, we detected no increase in the expression of activation markers CD69 or CD25 by 2D2 $CD4^+$ T cells (Fig. 5D-E), which argues against CS providing an antigenic stimulus for the MOG reactive T cells. However, the expressions of IFN-γ and IL-17A as assessed by MFI were increased in the $CD44^{hi}$ subfraction of 2D2 $CD4^+$ T cells, particularly after these cells were activated *ex vivo* with MOG p35-55 (Fig. 5F-G). These changes in cytokine production were not seen in 2D2 $CD4^+$ T cells in the spleens of CS-exposed mice (Fig. 5G), reinforcing the idea that the effects of CS on T cells are limited to $CD44^{hi}$ T cells and only within the CS-induced lung milieu.

Notably, during these prolonged CS exposures, we noted that some 2D2 mice developed a positive hindlimb clasping reflex upon tail elevation (Fig. 5H), which we previously described to correlate with mild T cell autoimmunity in the dorsal spinal cord white matter and nerve roots (29). To confirm development of autoimmunity, we harvested the spinal columns of three representative 2D2 mice that displayed a hindlimb clasping at symptom onset or remained asymptomatic and stained thoracic and lumbar spinal cord sections for CD45. This analysis revealed the expected sparse infiltration of $CD45^+$ cells in the dorsal white matter of hindlimb clasping in CS-exposed mice showing this reflex (Fig. 5I); however, the more prominent pathological finding was that 50% of dorsal root ganglions (DRGs) of hindlimb clasping mice were infiltrated with leukocytes (Fig. 5I). When AA-exposed mice were inspected that did not show hindlimb clasping, a significantly lowered proportion of DRGs were infiltrated (10% in AA, Chi-square=38.1, $p<0.05$), and no cells were observed in the dorsal spinal cord. Since the DRG is part of the peripheral nervous system and does not express MOG, this pathology is likely driven by the known cross-reactivity of 2D2 cells for the neuronal protein neurofilament-medium (29, 43). Together, these findings support the idea that

CS exposure in the lung has chemotactic activity on activated MOG p35-55-reactive T cells where the pro-inflammatory milieu acts to further amplify cytokine production by T cells that have previously received an antigen signal. This effect in 2D2 mice resulted with the development of mild neuro-autoimmunity.

Dendritic Cells and Macrophages Are More Mature in CS-Exposed Lungs and More Efficiently Prime MOG p35-55-Reactive Th Cells

The greater activation of T cells in CS-exposed male lungs led us to examine the maturation status of classical DCs (cDCs) and macrophages in the lungs in the context of the passive transfer EAE model. CD86 expression was detected at greater levels in cDCs in male mice with CS-exposure (*black panels*, Fig. 6A). In addition, both MHC-II and CD86 were upregulated with CS on macrophage populations in the lung (Fig. 6A). In case of these markers, a similar pattern of MHC-II and CD86 expression was seen in the females (*red panels*, in Fig. 6A).

We also investigated whether lung DCs from the CS-exposed lung had a greater capacity to prime MOG p35-55-reactive T cells *in vitro* as compared to AA-exposed lung DCs. To this end, $CD11c^+$ cells were isolated from digested lungs of CS- and AA-exposed mice and then set up in co-culture with 2D2 $CD4^+$ T cells in the presence and absence of MOG p35-55. Consistent with flow cytometry findings of a greater maturation status on CS-exposed DCs, we detected that a greater percentage of 2D2 $CD4^+$ T cells were activated, divided and became effector Th1 and Th17 $CD4^+$ T cells in the CS DC-T cell co-cultures (Fig. 6B-F). MOG p35-55 had to be included in the cultures to see this effect, further reinforcing the idea that the smoke particles do not serve as an antigenic stimulus for these $CD4^+$ T cells.

Certain Cytokines and Chemokines Are Upregulated More in Males With CS

Beyond MHC-II:peptide and co-stimulatory signals, DCs also provide type 3 (cytokine) signals to $CD4^+$ T cells. To gain insights on the changes in the lung cytokine environment with CS, we broadly profiled cytokine and chemokine levels in lysates prepared from the lungs of AA- and CS-exposed male and female mice. These lungs had been preserved from an experiment where male and female mice had been exposed in parallel to CS- or AA and were immunized with MOG p35-55/CFA (Fig. 6G).

Consistent with past studies using this CS-exposure regimen (27, 44-48), CS caused an upregulation of a number of cytokines known to be produced by cells of the innate immune system, the most prominent being IL-1α, IL-12p40, IL-33, GM-CSF; IL-6 and type I IFNs also tended to be upregulated with CS. We also detected higher levels of the B cell survival factor BAFF and the chemokine CXCL13 which is known to draw B cells into TLS (49). The Th2 cytokines (IL-4, IL-5) and IL-10 were not significantly altered. In addition, some chemokines known to attract monocytes/macrophages (CCL3), T cells (CXCL10), and eosinophils (eotaxin, CCL3) were upregulated with CS; CCL3 was increased in both sexes, eotaxin was increased only in the males, and CXCL10 was selectively increased in females (Fig. 6H). When comparing the males versus the females, some inflammatory factors tended to be upregulated more so in males; these included IL-3, IL-12p40, and IL-33 (Fig. 6G). IL-3 promotes survival of eosinophils which may help explain the more prominent accumulation of eosinophils in the male lungs with CS. Though IL-33 is known to promote the activation of lung ILC2s and type 2 immunity; in the presence of IL-12 caused by CS and influenza infection, it is reported to instead promote type 1 inflammation in the lungs (50). Thus, our cytokine signature can explain the greater effects of CS in promoting lung inflammation Th1/Th17 immunity in the males.

IL-12p40 Accounts for the Greater Effect of CS-Exposed DCs and CS-Exposed Lungs on Th1/Th17 Cytokine Production by MOG p35-55-Reactive Th Cells

The finding of increased IL-12p40, particularly in the male lung with CS resonated with the findings of greater expression of IFN-γ, IL-17, and GM-CSF by lung myelin-reactive Th cells. IL-12p40 is produced by lung $CD11b^+$ $CD11c^+$ cells (51) and has been documented to promote Th1 immunity through formation of IL-12p70 (p40/p35) and IL-12p40 homodimer (26, 52-54). As part of IL-23 (p40/p19), IL-12p40 promotes Th17 cell lineage stabilization and expression of GM-CSF (52), another cytokine that is essential to EAE development (55-58). To investigate whether IL-12p40 production is the factor that accounts for the increased activity of the lung DCs on 2D2 cells, we set up DC:$CD4^+$ T cell cultures with MOG p35-55 as done previously except we also including a neutralizing IL-12p40 antibody or isotype control antibody in the co-cultures. We found that wells with CS-exposed DCs that were provided anti-IL-12p40 showed reduced T

cell proliferation, expression of activation markers, and IFN-γ and IL-17 expression compared to those treated with isotype control antibody. By contrast, there was very little impact of anti-IL-12p40 treatment in the co-cultures that contained DCs from the AA-exposed mice (Fig. 7A-D). These findings suggest that excess production of IL-12p40 or IL-12p40 cytokines by lung CD11c^{+} cells during CS exposure may have contributed to greater T cell activation and Th1/Th17 cytokine production that we saw in the lung.

We also repeated passive EAE studies in CS or AA-exposed mice, but provided two doses of anti-IL12p40 or isotype control antibody intranasally on day -2 and at day 1 post-transfer of the cells, a time when myelin-reactive Th cells should be first trafficking to the lung. This dose and route of anti-IL-12p40 administration was effective at depleting lung, but not spleen IL-12p40 (Supplementary Fig. 1). We then analyzed the donor CD45.1^{+} MOG p35-55-reactive CD4^{+} T cells in lung at day 4 post-transfer by flow cytometry. As before, CS-exposure induced a greater accumulation of total CD45^{+} cells, MOG-reactive Th17 effector cells (CD45.1^{+}CD4^{+}CD44^{hi}IL-17^{+}) and those-co-producing IL-17 and GM-CSF (Fig. 7E-I). In CS-exposed mice, anti-IL-12p40 significantly reduced the accumulation of transferred MOG p35-55-reactive IL-17 and IL-17 and GM-CSF co-producing T cells (Fig. 7E, H-I). On the other hand, anti-IL-12p40 had minimal effects in AA-exposed mice (Fig. 7E-I). These findings confirm a role for IL-12p40 in the CS-exposed lung in both the recruitment and further education of primed MOG p35-55-reactive Th cells.

DISCUSSION

The mechanisms that drive the initiation of MS are unknown; however, the genetic and lifestyle triggers are well-understood. Learning the biology linking these factors to MS may not only shed light on the underlying immune mechanisms, but also provide new ways of intervening in this disease. Cigarette smoking promotes MS development, especially in men. Epidemiological studies have also suggested an interaction between CS exposure and carriage of the MHC-II MS risk haplotype on disease risk, suggesting that smoking promotes Th autoimmunity (59). Here, we used a whole-body passive exposure system to demonstrated in mice that CS exposure induced increased lung T

and B cell clustering and DC maturation, and promoted a pro-inflammatory environment in the lung that led to the hyper-activation of myelin-specific Th cells. Our studies further identified that elevated lung IL-12p40 was a driving factor in this effect of CS on T cells in the lung. In 2D2 mice, these effects on $CD44^{hi}CD4^{+}$ T cells in the lung were associated with heightened neuroimmunity. These findings thus provide a potential mechanism for how CS exposure promotes T cell autoimmunity in MS.

We explored the effect of CS on EAE development in three different EAE models: active EAE, IL-23-induced Th17 passive transfer EAE, and TCR transgenic mice that had dual reactivity for MOG p35-55 and neurofilament medium (NF-M p18-30). In the case of active EAE, where the presence of heat-killed tuberculosis in the adjuvant promotes a strong Th1 response, CS exposure enhanced IFN-γ and TNF production by MOG p35-55 Th cells in the peripheral lymphoid organs. We speculate, based on past studies that characterized T cell trafficking in passive transfer EAE (37), that the MOG p35-55-reactive Th cells acquired this greater capacity to produce IFN-γ because they had already trafficked through the pulmonary circuit at the time of sampling. Greater IFN-γ expression was also observed in the host $CD44^{hi}CD4^{+}$ cells recruited to the lung during passive transfer EAE and in $CD44^{hi}CD4^{+}$ cells in the CS-exposed 2D2 mice. In the case of the Th17 transfer EAE, CS promoted greater T cell expression of activation markers and IL-17 and GM-CSF, which are cytokines that these cells had been programmed to make with IL-23 treatment. Together, these findings are consistent with past studies that CS exposure can promote Th1/Th17 inflammation in the lungs of mice (40, 48). They further align with findings in humans that cigarette smoking can promote type I inflammatory markers in the BAL and sputum and increase circulating $IFN\text{-}\gamma^{+}IL\text{-}17^{+}$ and $CXCR3^{+}$ (Th1-like) memory T cells (60, 61). Furthermore, our finding in 2D2 mice that cytokine-enhancing effects of CS on 2D2 $CD4^{+}$ T cells were only seen in $CD44^{hi}$ fraction, and only in the lung, further emphasize that the education of the T cells by CS-exposed DCs is likely restricted to this site. We found that DCs from CS-exposed lungs had a greater ability to prime myelin-reactive Th1 and Th17 cells. This is in accordance with previous works showing that CS activates lung DCs, triggering type-1 and -3 inflammation. Lung DCs can activate Th1 and Th17 responses in human emphysema (62), and, in a mouse model, CS-activated DCs can transfer emphysema

by inducing pathogenic Th17 cells (63). Similar to our findings, CS has also been shown to activate the production of IL-1β and IL-23 by cDCs, which in turn trigger type-3 inflammation, by polarizing ILCs into IL-17-producing ILC3s (64). Finally, the CS-induced increase of lung cDCs may be related with the TLS observed in CS-exposed lungs, as lung cDCs have been shown to promote the formation of TLS by priming T follicular helper cells in chronic obstructive pulmonary disease (COPD) (65). Altogether, these findings suggest that the CS-treated lungs amplify the activation and cytokine production by T effector cells as they circulate through this organ, which in the case of the 2D2 mice, tipped the balance towards autoimmunity.

Our finding that neutralizing IL-12p40 in the airways inhibited the ability of CS lung DCs to recruit the myelin-specific T cells to the lung and the finding that anti-IL-12p40 neutralization prevented the ability of the CS-exposed DCs to promote Th1 or Th17 cytokine production aligns with the known roles of IL-12p40 and IL-12 family cytokines on Th cells (26, 52, 54). Both IL-12p70 and the IL-12p40 homodimer promote IFN-γ production (26, 54), IL-23 promotes stabilization of the Th17 lineage (52), and IL-12p70 and IL-23 can promote T cell production GM-CSF (52, 66). Though our cytokine profiling assay revealed a greater upregulation of IL-12p40 relative to the IL-23 or IL-12p70, we speculate that a combination of these cytokines affected the T cells. This is because only IL-12p70 and IL-23, but not the IL-12p40 have known roles in promoting GM-CSF production (52, 66) and because treatment with the IL-12p40 monomer actually inhibits GM-CSF (67). Furthermore, past studies have described roles for IL-12p70 and IL-23 in the development of other CS-associated pathologies including fibrosis (68) and emphysema (69). Resolving the individual contributions of IL-12p70, IL-23, and IL-12p40_2 will require employing mice that are singly or doubly deficient in the protein subunits, as has been done in the context of infection models (70).

Our findings that anti-IL-12p40 combatted myelin-specific Th cell cytokine production in the lungs of male mice exposed to CS also brings this cytokine back into the limelight within the MS treatment landscape. In light of early findings in mice that IL-12p40 was absolutely required for EAE development (71) and that IL-12 and IL-23 confers encephalitogenic properties to T helper cells (72), anti-IL12/23 p40 antagonistic antibodies were tested in phase 2 clinical trials in MS. A trial testing subcutaneous

utekinumab in patients with MS was disappointing and failed to show efficacy in reducing the appearance of new gadolinium- (Gad) enhancing lesions in the brain (56). Another trial testing briakinumab did have efficacy in reducing Gad-enhancing lesions and relapses, but the antibody was not developed further due to the relatively modest effects compared to other treatments. Notably, these trials did not segregate data by sex or smoking status, thus we do not know whether the anti-IL-12p40 had a selective benefit in smokers. Though we could not find data reporting on IL-12p40 in the BAL of human smokers, one study did report finding increased levels of IL-12p40 in the serum of human smokers (60) providing some rationale to test anti-IL-12p40 as an add-on therapy for humans with MS who smoke.

The cytokine profiling assay in lung homogenates from CS-exposed mice also revealed a prominent increase in IL-33 and IL-1α and a significant increase in GM-CSF with CS exposure. This cytokine signature is very similar to that described by past studies in mice by the Stampfli group using this same smoke-exposure system and regimen. These authors found that both IL-1α and GM-CSF play a role in the early inflammatory circuit that is involved in the recruitment of leukocytes to the lung during CS (44, 45). These studies also demonstrated that neutralization of IL-1α inhibited the induction of GM-CSF (44). Follow-up studies that focused on the function of GM-CSF in lung inflammation showed that neutralization of GM-CSF prevented the early accumulation of DCs, activation of $CD8^+$ T cells, and induction of IL-12p40 (45). These studies therefore places GM-CSF and IL-1α upstream of IL-12p40 in CS-induced lung inflammation. In addition, past studies have described roles for IL-1α and IL-12p40 in shifting type 2 to type 1 inflammation during CS (50). Though IL-33 is best known for its role in promoting type 2 innate lymphoid cell (ILC2) expansion in the female lung during states of health and allergy (73), in the context of CS-exposure and influenza infection, induction of IL-33 coupled with downregulation of the IL-33 receptor ST2 on ILC2s instead promotes macrophage and DC activation, as well as type 1 immunity (50). Along a similar theme, a study in humans showed that IL-12 together with IL-1 induced the trans-differentiation of human ILC2 to ILC1 cells (74). Our finding that both IL-33 and IL-12p40 were more prominently elevated in the male lungs with CS and the finding that Th2 cytokines were not altered, suggests that this axis of inflammation may be

turned on to a greater extent so in males during CS exposure. Though anti-IL-33 was shown in a trial to have a signal in improving lung function in a subset of patients with COPD that have a high risk for exacerbations (75); the expression of this cytokine is also reported to be reduced in the lungs of current smokers who do not have COPD (76), making it unclear whether this cytokine is also a candidate therapy for treating lung inflammation in smokers.

We also detected T cell/B cell microclusters in the lungs of mice with 8 weeks of CS exposure, which are a prelude to the more organized TLS structures that can develop in mice with more prolonged CS exposures (32) or in humans with COPD (77). We further provided evidence that transferred CD45.1^{+} MOG p35-55-reactive Th cells could home to these microclusters, suggesting that these could be sites where the MOG p35-55 T cells are engaging DCs to become activated and produce cytokines. Past studies showed that TLS formation in the lungs could be prevented by co-administration of a BAFF-Fc reagent (32), which raised the prospect that targeting TLS formation could be an approach to consider for treating lung inflammation in smokers. Though interstitial lung disease with lymphocytic infiltrates develops in patients with RA (78), whether this also occurs in MS patients who smoke is unclear and should be investigated in future studies.

Our study also brings additional attention to the lung-brain axis in the regulation of MS-related autoimmunity. A connection between the lung and brain was first suspected when epidemiology studies found a temporal association between respiratory tract infections and MS relapses (79-84) and first clinical presentation of this disease (85). However, concrete evidence that the lung environment could promote CNS autoimmunity did not come until studies in rodents demonstrated that myelin-reactive T cells traffic through the BALT and lung draining lymph nodes on their way to the CNS during EAE (37). This study also showed that this residence in the lung and BALT was important for the acquisition of chemokine receptors and adhesion molecules that are required for successful transmigration of the myelin-reactive T cells into the CNS (37). Beyond this, murine studies have provided evidence that the lung commensal and microbial environment can modulate CNS autoimmunity. For example, intranasal infection of mice with PR8 influenza exacerbates EAE by promoting a Th1 cytokine

response by myelin-reactive Th cells in the lung environment (86). When 2D2 mice are infected with this same virus, it triggers a mild CNS autoimmune disease characterized by the infiltration of leukocytes into the spinal nerve roots (77), reminiscent of the disease phenotype that we observed after CS exposure. Manipulating the lung flora towards LPS-enriched phyla using neomycin has been shown to ameliorate EAE by lowering the activation state of microglia in the CNS (87). Finally, delivery of antigen-coated microparticles to the lung has the effect of recruiting and tolerizing myelin-reactive Th cells to treat EAE (88).

Study Limitations

Despite testing CS in different EAE models, we were unable to demonstrate that CS worsened myelin-specific CNS disease. Having such a model would be an important requisite for pre-clinical testing of therapies that aim to decrease lung inflammation in MS patients who smoke. A major barrier to this goal was that the CS-induced lung inflammation produced a strong chemotactic pull on the myelin-reactive Th cells, which slowed their entry to the CNS. A similar recruitment of immune cells to the lung and delay of EAE has been seen with other CS-exposure protocols (34) as well as after LPS installation in the airway in mice (86). Furthermore, a ying-yang effect of CS exposure in both promoting yet also delaying onset of autoimmunity has been seen in lupus in MRL-*lpr/lp*r mice, where CS exposure delays the appearance of autoantibodies by 2 weeks, but also exacerbates the production of anti-chromatin IgM and IgG antibodies from 20 weeks of age and onwards (89). In future studies, we will experiment with lowering the cigarette dose and the time of the exposure to see if we can still maintain the pro-encephalitogenic activities of the lung DC and at the same time lower the chemotactic activities of the inflamed lung on the T myelin-reactive cells.

In conclusion, our findings demonstrate that myelin-reactive Th cells traffic to the CS-exposed lung where they acquire signals including IL-12p40 that amplify the production of cytokines, thereby providing a mechanism for how CS promotes autoimmunity.

Acknowledgements

This work was funded by grants from the National MS society (to M.S., C.R., S.E.D.) and MS Canada (S.E.D., C.S., W.L.) and start-up funds from the St. Michael's Hospital Foundation (S.E.D.). We thank Dr. Monika Lodyga, Dr. Caterina DiCiano-Oliveira, Dr. Xiaofeng Lu from research facilities at St. Michael's hospital for help with training personnel in imaging and flow cytometry. We thank staff at the Toronto Center for Phenogenomics for evaluation of lung pathology and embedding and sectioning of our tissues. We thank the staff of the University Health Network animal facility for their expert care of animals. We thank Dr. Alan Lazarus and Dr. Veronica Miron for helpful discussions and mentorship.

Figure Legends

Figure 1. Exposure of mice to bouts of passive CS over eight weeks raises cotinine levels and induces immune cell infiltration in the lung. A) Serum cotinine levels in male C57BL/6J mice exposed to either CS or ambient air (AA), measured less than one 1 h post-exposure. Sections of lungs of AA- and CS-exposed males were stained for CD45 and the number of $CD45^+$ cells (B), the mean area of clusters of $CD45^+$ cells in μM^2 (C), and area of the lungs occupied by $CD45^+$ clusters in mm^2 (D) was measured. E) Representative CD45 antibody-stained sections of lungs in AA- and CS-exposed males, showing immune cell clusters located close to blood vessels and bronchioles. F-H) Immune populations were identified by flow cytometry in lungs of AA- and CS-exposed mice using this gating strategy (pre-gated on live singlets) (F); total numbers of $CD45^+$ cells in the lung (G) and of the immune cell populations indicated (H). Data are presented as mean ± SEM. Data points are individual mice from one experiment that is representative of three performed. * $p \leq 0.05$ between groups as determined by two-tailed Mann-Whitney U test (A-G) or 2-way ANOVA followed by Bonferroni post-hoc test (H). In (H), black asterisks indicate $p \leq 0.05$ when comparing AA- and CS-exposed males, and red asterisks indicate statistical significance between female groups.

Figure 2. Chronic exposure of mice to cigarette smoke (CS) enhances MOGp35-55 specific Th1 responses. Ambient air (AA)- or CS-exposed male C57BL6/J mice were

immunized with MOG p35-55/CFA and the recall cytokine and proliferative responses of cells were assessed 9 days later in isolated spleen and draining lymph node (dLN) mononculear cells. A-B) Levels of Th1, Th17 and Th2 cytokines in supernatants of MOG_{35-55}-stimulated (0-10 µg/mL) cell cultures from spleens (A) and dLNs (B). C-E) Division of splenic $CD4^+$ $CD44^{high}$ T cells after stimulation in the presence/absence of MOG p35-55 ex vivo as assessed by CFSE dilution. Representative plots of dividing $CD4^+$ T cells (C), and frequency (D) and total numbers (E) of dividing $CD4^+$ $CD44^{high}$ T cells. Data in A, B, are mean ± SEM of triplicate wells of cultures from pooled mice and are representative of three independent experiments in males and two independent experiments in females. Data points in C are individual mice from one experiment that is representative of 3 proliferation assays performed. *different between groups as determined by Mann-Whitney (A,B) or 2-way ANOVA and Bonferroni post hoc test ($p \leq 0.05$).

Figure 3. Cigarette smoke (CS) exposure decreases EAE severity in males. A-H) Male (in black) and female (in red) C57BL/6J mice were exposed to 8-10 weeks of ambient air (AA) or CS prior to active EAE induction according to the schematic in (A). EAE curves (B), cumulative EAE scores (C), peak EAE scores (D) and day of EAE onset (E). Immune infiltration (number of $CD45^+$ cells/mm^2 of white matter (WM)) (F) and percentage of demyelination (G) at the level of the thoracic spine in AA- or CS-exposed EAE mice, and representative microphotographs of immune infiltration ($CD45^+$; top panel) and demyelination (Luxol Fast Blue [LFB]; bottom panel) in thoracic spinal cord (H). I-K) Male C57BL/6J mice were exposed to 8-10 weeks of AA or CS, followed of a 4.5 day washout period prior to active EAE induction according to the schematic in (I). EAE scores (J) and cumulative EAE scores (K) of. Data are presented as mean ± SEM of individual mice from one experiment. *Different ($p \leq 0.05$) between groups as determined by two-way ANOVA and Bonferroni post hoc test (B, J) or by two-tailed Mann-Whitney U test (B-G, K).

Figure 4. Myelin-reactive T cells are stalled and hyperactivated in cigarette smoke (CS)-exposed lungs. Passive EAE was induced in male C57BL/6J mice that had been exposed to ambient air (AA) and CS for 8 weeks, by transferring in IL-23-polarized, MOG_{35-55}-reactive female T cells from unexposed donor mice. A-B) EAE scores (A) and

day of EAE onset (B) in AA- and CS-exposed EAE recipients. C-M) Passive EAE was similarly induced, but instead by transferring IL-23-polarized, MOG_{35-55}-reactive T cells from unexposed donor $CD45.1^+$ mice (C-G; L-M) or from unexposed donor C57BL/6J (H-K) to AA- and CS-exposed C57BL/6J ($CD45.2^+$) mice; recipient mice were euthanized when both groups reached the peak of the disease (gray arrow in (A)) to analyze donor cell infiltration into the CNS (C-G) and lungs (L-M), and to assess MOG_{35-55}-reactive T cells in the lungs and spleens (H-K); to assess cytokine production, cells were stimulated *in vitro* with MOG_{35-55} for 12 hours, with GolgiStop added in the last 5 h. Representative FACS plots of donor $CD45.1^+$ cells (C), total numbers of mononuclear cells (D) and of $CD45.1^+CD4^+$ T cells (E); frequencies of MOG_{35-55}-reactive $CD45.1^+CD4^+CD44^{high}$ T cells producing IL-17 or IL17 and GM-CSF (F); and ratio of encephalitogenic T cells ($CD45.1^+CD4^+CD44^{high}IL17^+$) vs. total donor cells ($CD45.1^+$) (G) isolated from the CNS of EAE $CD45.2^+$ recipients. Total numbers of $IL17^+$, $IL17^+IFN\text{-}\gamma^+$, and $IFN\text{-}\gamma^+$ $CD4^+$ T cells in lungs (H) and representative FACS plots (I); total numbers of $IL17^+$, $IL17^+IFN\text{-}\gamma^+$, and $IFN\text{-}\gamma^+$ $CD4^+$ T cells in spleen (J), and IL-17 and GM-CSF median fluorescence intensities (MFIs) of lung MOG_{35-55}–reactive $IL17^+$ $IFN\text{-}\gamma^-$ $CD4^+$ T cells (K). CD25, CD69 and PD-1 expression by donor $CD45.1^+CD4^+CD44^{high}$ T cells in the lungs (L), and the homing of the donor $CD45.1^+$ cells to the perivascular and peribronchiolar immune clusters in the lungs (M). Data in A-B are presented as mean ± SEM of individual mice from one representative experiment of at least four that were performed in male and two in female mice. Data examining CNS cells in C-H are mean ± SEM of individual mice from 1 experiment. Data investigating cytokines and activation markers in the lung are mean + SEM of individual mice and are representative of 4 independent experiments that were performed. *: $p \leq 0.05$ between groups as determined by two-way ANOVA and Bonferroni post hoc test (A, H, J) or by two-tailed Mann-Whitney U test (B, D-G, K-L).

Figure 5. Cigarette smoke (CS) enhances cytokine production by 2D2 $CD4^+$ T cells in the lungs and enhances neuroimmunity. Female and male 2D2 mice aged 6-7 weeks were exposed to ambient air (AA) or CS for 8 weeks. Mice were followed for clinical signs and at endpoint flow cytometry was performed to examine the profile of 2D2 CD4+ T cells in the lung and spleen. A) Total number of cells in lungs. B) Total

number of myelin-reactive, transgenic TCR-expressing, 2D2 $CD4^+$ T cells in the lungs. C) Distribution of naïve ($CD44^-$ $CD62L^+$), central memory ($CD44^+$ $CD62L^+$) and effector memory ($CD44^+$ $CD62L^-$) phenotypes in of myelin-reactive, transgenic TCR-expressing, 2D2 $CD4^+$ T cells in the lungs. D) Median fluorescence intensity (MFI) of CD25 in memory ($CD44^{high}$) and naïve ($CD44^{low}$) myelin-reactive, transgenic TCR-expressing, 2D2 $CD4^+$ T cells in the lungs. E) MFI of CD69 in memory ($CD44^{high}$) and naïve ($CD44^{low}$) myelin-reactive, transgenic TCR-expressing, 2D2 $CD4^+$ T cells in the lungs. F) MFI of IFN-γ and IL-17 by lung cytokine-producing, memory 2D2 $CD4^+$ T cells cultured *in vitro* with/without MOG_{35-55}. G) Representative FACS histograms of IFN-γ and IL-17 production by lung cytokine-producing, memory 2D2 $CD4^+$ T cells. H) Frequency of 2D2 mice developing CNS autoimmunity after exposure. I) Representative CD45 staining showing sparse immune cell infiltration in the spinal cord, the dorsal root ganglion and spinal nerve roots CS-exposed 2D2 mice. Flow data are presented as mean ± SEM of individual mice (n=8-9/group) from one experiment. Clinical data are from two consecutive cohorts exposed for 8 weeks (n=9-21/group/sex). *Different ($p \leq 0.05$) between groups as determined by two-tailed Mann-Whitney U test (A, B, C, E), $\chi 2$ test (C, H), and two-way ANOVA and Bonferroni post hoc test (F).

Figure 6. Cigarette smoke (CS) increases the activation of antigen presenting cells (APCs) and proinflammatory molecules in lungs. Male and female C57BL/6J mice were exposed to ambient air (AA) or CS for 8-10 weeks and were transferred with MOG p35-55 reactive T cells. Lungs were harvested at a time when AA-exposed mice had developed EAE and CS-exposed mice were still asymptomatic. A) Representative FACS plots of the expression of activation markers (CD86, MHC-II) in APCs isolated from male and female C57BL/6J mice exposed to ambient air (AA) or CS. B-F) Dendritic cells (DCs) isolated from lungs of AA- and CS-exposed male C57BL/6J mice were cultured in presence of MOG_{35-55} (0-10 µg/mL) with myelin-reactive $CD4^+$ T cells isolated from spleens of 2D2 male mice. Proliferation (B) of 2D2 $CD4^+$ T cells, expression of CD25 (C), CD69 (D), IFN-γ (E) and IL-17 (F) on memory 2D2 $CD4^+$ T cells. G-H) Cytokine (G) and chemokine (H) levels in lung tissue. Analytes were measured in pg/mL and expressed as pg/mg of tissue. Data points are individual mice from two experiments where male and female mice were exposed to CS- or AA-in

parallel and immunized with MOG p35-55/CFA *: p≤0.05 between groups as determined by 2-way ANOVA and Bonferroni post hoc test. Black asterisks indicate p≤0.05 when comparing AA- and CS-exposed males, red asterisks indicate statistical significance for female groups, and blue asterisks indicate statistical significant interactions (sex by exposure) by 2-way ANOVA.

Figure 7. IL-12p40 is an important pro-inflammatory mediator in the lung that drives the hyperactivation of $CD4^+$ T cells. A-D) AA- and CS-exposed lung DCs were cocultured with splenic myelin-reactive 2D2 $CD4^+$ T cells in presence/absence of MOG_{35-55} (5 µg/mL) with a blocking anti-IL12p40 antibody or isotype control antibody. Proliferation (A) of 2D2 $CD4^+$ T cells, expression of CD25 (B), IFN-γ (C) and IL-17 (D) in $CD44^{hi}$ 2D2 $CD4^+$ T cells. E-I) Passive EAE was induced by transferring IL-23-polarized, MOG_{35-55}-reactive T cells from unexposed donor $CD45.1^+$ mice into AA- and CS-exposed male C57BL/6J ($CD45.2^+$) mice; 2 days prior to, and 1 day after the adoptive transfer, recipient mice received a blocking anti-IL12p40 or isotype control antibody intranasally (125 µg/animal/dose). Representative FACS plots of donor cells ($CD45.1^+$) (E), numbers of total cells (F), donor $CD4^+$ T cells (G) and MOG_{35-55}-reactive donor $CD44^{high}CD4^+$ T cells producing IL-17 (H) and IL-17 with GM-CSF (I) located in the lungs of recipient CD45.2 mice. Data presented are mean ± SEM of individual mice. *: p≤0.05 between groups as determined by two-way ANOVA and Bonferroni post hoc test.

Supplementary Figure 1. Blockade of lung IL-12p40 production by intranasal vs intratracheal administration of a blocking anti-IL12p40 antibody. A blocking anti-IL12p40 antibody (0-250 µg/animal) was administered either intranasally or intratracheally to male C57BL/6J mice; three days after the administration, IL-12p40 levels were measured in tissue lysates of lungs (A), small intestine (B) and spleen (C). Data are presented as mean ± SEM of individual mice from one experiment *: p≤0.05 between groups as determined by two-way ANOVA and Bonferroni post hoc test; asterisks show statistical significance between 0 and the marked concentration of antibody for intranasal (black asterisks) and intratracheal (grey asterisks) administration.

Supplementary Figure 2. B and T cells accumulate in perivascular and peri-bronchial clusters in cigarette smoke (CS)-exposed lungs. Dual CD3 (DAB) and B220 (Vector Blue) staining in lung sections of ambient air (AA) (in A) and CS-exposed (B-D) mice. A shows the presence of scattered T cells in the AA-exposed lung. B-D) Examples of pathology in the CS-exposed lungs. B) Shows a larger and smaller lymphocytic infiltrate containing T cells and B cells. C) Shows a less organized lymphocytic structure around the airway with T and B cells present. D) Shows an example of T cell cluster with no B cells present.

Supplementary Figure 3. Chronic exposure to cigarette smoke (CS) has milder effects in females in passive EAE studies. A-B) Ambient air (AA)- or CS-exposed female C57Bl/6J mice were immunized with MOG_{35-55} to assess the *in vitro* cytokine and proliferative recall responses of cells isolated from spleen and draining lymph nodes (dLNs) 9 days after immunization. Levels of Th1, Th17 and Th2 cytokines in supernatants of MOG_{35-55}-stimulated (0-10 µg/mL) cell cultures from spleens (A) and dLNs (B). These data are from one experiment and are representative of two experiments that were performed. C-D) Passive EAE was induced in female C57BL/6J mice previously exposed to ambient air (AA) and CS for 8 weeks, by transferring IL-23-polarized, MOG_{35-55}-reactive female T cells from unexposed donor mice); to assess cytokine production, cells were stimulated *in vitro* with MOG_{35-55} for 12 hours. EAE curves (C), and IL-17 and GM-CSF median fluorescence intensity (MFI) in MOG_{35-55}-reactive IL-17^{+}IFN-γ^{-}CD4^{+} cells (D). F-I) Passive EAE was similarly induced, but transferring IL-23-polarized, MOG_{35-55}-reactive T cells from unexposed donor CD45.1^{+} mice to AA- and CS-exposed C57BL/6J (CD45.2^{+}) mice. F) MFI of CD25 in CD45.1^{+}CD4^{+}CD44^{high} donor cells. G) MFI of CD69 in CD45.1^{+}CD4^{+}CD44^{high} donor cells. H) MFI of CD25 in CD45.1^{-}CD4^{+}CD44^{high} resident cells. I) MFI of CD69 in CD45.1^{-}CD4^{+}CD44^{high} resident cells. Data in A-B are mean ± SEM of triplicate wells of cultures from pooled mice and are representative of three independent experiments. Data points in C-D are individual mice from one experiment that is representative of 2 performed. Data points in C-D are individual mice from one experiment. *: $p \leq 0.05$ between groups as determined by 2-way ANOVA and Bonferroni post hoc test (A-C) or two-tailed Mann-Whitney U test (D-I).

1017

REFERENCES

1. Taylor AL, Bettcher, D.W. WHO Framework Convention on Tobacco Control: a global "good" for public health. *Bulletin of the World Health Organization, 2000, 78 (7).* 2000:920-9.
2. WHO global report on trends in prevalence of tobacco use 2000-2025, third addition. 2019:1-99
3. Dai X, Gakidou E, and Lopez AD. Evolution of the global smoking epidemic over the past half century: strengthening the evidence base for policy action. *Tob Control.* 2022;31(2):129-37.
4. Miller FW. The increasing prevalence of autoimmunity and autoimmune diseases: an urgent call to action for improved understanding, diagnosis, treatment, and prevention. *Curr Opin Immunol.* 2023;80(102266.
5. Bach JF. The effect of infections on susceptibility to autoimmune and allergic diseases. *The New England journal of medicine.* 2002;347(12):911-20.
6. Perricone C, Versini M, Ben-Ami D, Gertel S, Watad A, Segel MJ, Ceccarelli F, Conti F, Cantarini L, Bogdanos DP, et al. Smoke and autoimmunity: The fire behind the disease. *Autoimmun Rev.* 2016;15(4):354-74.
7. Kallberg H, Ding B, Padyukov L, Bengtsson C, Ronnelid J, Klareskog L, Alfredsson L, and Group ES. Smoking is a major preventable risk factor for rheumatoid arthritis: estimations of risks after various exposures to cigarette smoke. *Ann Rheum Dis.* 2011;70(3):508-11.
8. Hedstrom AK, Olsson T, and Alfredsson L. Smoking is a major preventable risk factor for multiple sclerosis. *Mult Scler.* 2016;22(8):1021-6.
9. Hedstrom AK, Baarnhielm M, Olsson T, and Alfredsson L. Tobacco smoking, but not Swedish snuff use, increases the risk of multiple sclerosis. *Neurology.* 2009;73(9):696-701.
10. Sugiyama D, Nishimura K, Tamaki K, Tsuji G, Nakazawa T, Morinobu A, and Kumagai S. Impact of smoking as a risk factor for developing rheumatoid arthritis: a meta-analysis of observational studies. *Annals of the rheumatic diseases.* 2010;69(1):70-81.
11. Palacios N, Alonso A, Bronnum-Hansen H, and Ascherio A. Smoking and increased risk of multiple sclerosis: parallel trends in the sex ratio reinforce the evidence. *Ann Epidemiol.* 2011;21(7):536-42.
12. Healy BC, Ali EN, Guttmann CR, Chitnis T, Glanz BI, Buckle G, Houtchens M, Stazzone L, Moodie J, Berger AM, et al. Smoking and disease progression in multiple sclerosis. *Archives of neurology.* 2009;66(7):858-64.
13. Ramanujam R, Hedstrom AK, Manouchehrinia A, Alfredsson L, Olsson T, Bottai M, and Hillert J. Effect of Smoking Cessation on Multiple Sclerosis Prognosis. *JAMA Neurol.* 2015;72(10):1117-23.
14. Zivadinov R, Weinstock-Guttman B, Hashmi K, Abdelrahman N, Stosic M, Dwyer M, Hussein S, Durfee J, and Ramanathan M. Smoking is associated with increased lesion volumes and brain atrophy in multiple sclerosis. *Neurology.* 2009;73(7):504-10.
15. Alshehri E, Cohen JA, Ontaneda D, Nakamura K, Husak S, Love TE, Fox RJ, Briggs FB, and Conway DS. The impact of cigarette smoking on cognitive processing speed and brain atrophy in multiple sclerosis. *Mult Scler.* 2023;29(7):846-55.
16. Tanasescu R, Constantinescu CS, Tench CR, and Manouchehrinia A. Smoking cessation and the reduction of disability progression in Multiple Sclerosis: a cohort study. *Nicotine Tob Res.* 2017.
17. Hedstrom AK, Hossjer O, Katsoulis M, Kockum I, Olsson T, and Alfredsson L. Organic solvents and MS susceptibility: Interaction with MS risk HLA genes. *Neurology.* 2018;91(5):e455-e62.

18. Moutsianas L, Jostins L, Beecham AH, Dilthey AT, Xifara DK, Ban M, Shah TS, Patsopoulos NA, Alfredsson L, Anderson CA, et al. Class II HLA interactions modulate genetic risk for multiple sclerosis. *Nat Genet.* 2015;47(10):1107-13.
19. Karlson EW, Chang SC, Cui J, Chibnik LB, Fraser PA, De Vivo I, and Costenbader KH. Gene-environment interaction between HLA-DRB1 shared epitope and heavy cigarette smoking in predicting incident rheumatoid arthritis. *Annals of the rheumatic diseases.* 2010;69(1):54-60.
20. Hedstrom AK, Sundqvist E, Baarnhielm M, Nordin N, Hillert J, Kockum I, Olsson T, and Alfredsson L. Smoking and two human leukocyte antigen genes interact to increase the risk for multiple sclerosis. *Brain.* 2011;134(Pt 3):653-64.
21. Hedstrom AK, Baarnhielm M, Olsson T, and Alfredsson L. Exposure to environmental tobacco smoke is associated with increased risk for multiple sclerosis. *Mult Scler.* 2011;17(7):788-93.
22. Speyer CB, and Costenbader KH. Cigarette smoking and the pathogenesis of systemic lupus erythematosus. *Expert Rev Clin Immunol.* 2018;14(6):481-7.
23. Barbhaiya M, Tedeschi SK, Lu B, Malspeis S, Kreps D, Sparks JA, Karlson EW, and Costenbader KH. Cigarette smoking and the risk of systemic lupus erythematosus, overall and by anti-double stranded DNA antibody subtype, in the Nurses' Health Study cohorts. *Ann Rheum Dis.* 2018;77(2):196-202.
24. Conforti A, Di Cola I, Pavlych V, Ruscitti P, Berardicurti O, Ursini F, Giacomelli R, and Cipriani P. Beyond the joints, the extra-articular manifestations in rheumatoid arthritis. *Autoimmun Rev.* 2021;20(2):102735.
25. Faigle W, Cruciani C, Wolski W, Roschitzki B, Puthenparampil M, Tomas-Ojer P, Selles-Moreno C, Zeis T, Jelcic I, Schaeren-Wiemers N, et al. Brain Citrullination Patterns and T Cell Reactivity of Cerebrospinal Fluid-Derived CD4(+) T Cells in Multiple Sclerosis. *Front Immunol.* 2019;10(540.
26. Drohomyrecky PC, Doroshenko ER, Akkermann R, Moshkova M, Yi TJ, Zhao FL, Ahn JJ, McGaha TL, Pahan K, and Dunn SE. Peroxisome Proliferator-Activated Receptor-delta Acts within Peripheral Myeloid Cells to Limit Th Cell Priming during Experimental Autoimmune Encephalomyelitis. *J Immunol.* 2019;203(10):2588-601.
27. Botelho FM, Gaschler GJ, Kianpour S, Zavitz CC, Trimble NJ, Nikota JK, Bauer CM, and Stampfli MR. Innate immune processes are sufficient for driving cigarette smoke-induced inflammation in mice. *Am J Respir Cell Mol Biol.* 2010;42(4):394-403.
28. Ucciferri CC, Gower A, Alvarez-Sanchez N, Whetstone H, Ramaglia V, Gommerman JL, Brand-Arzamendi K, Schneider R, and Dunn SE. Scoring Central Nervous System Inflammation, Demyelination, and Axon Injury in Experimental Autoimmune Encephalomyelitis. *J Vis Exp.* 2024204).
29. Cahill LS, Zhang MA, Ramaglia V, Whetstone H, Sabbagh MP, Yi TJ, Woo L, Przybycien TS, Moshkova M, Zhao FL, et al. Aged hind-limb clasping experimental autoimmune encephalomyelitis models aspects of the neurodegenerative process seen in multiple sclerosis. *Proc Natl Acad Sci U S A.* 2019;116(45):22710-20.
30. Ucciferri CC, Gower, A., Alvarez-Sanchez, N., Whetstone, H., Ramaglia, R., Gommerman, J.L., Brand-Arzamendi, K., Schneider, R. and Dunn, S.E. . Scoring Central Nervous System Inflammation, Demyelination, and Axon Injury in Experimental Autoimmune Encephalomyelitis. *Journal of Visualized Experiments.* 2023;in press(
31. Cordeiro B, Ahn JJ, Gawde S, Ucciferri C, Alvarez-Sanchez N, Revelo XS, Stickle N, Massey K, Brooks DG, Guthridge JM, et al. Obesity intensifies sex-specific interferon signaling to selectively worsen central nervous system autoimmunity in females. *Cell Metab.* 2024.
32. Morissette MC, Jobse BN, Thayaparan D, Nikota JK, Shen P, Labiris NR, Kolbeck R, Nair P, Humbles AA, and Stampfli MR. Persistence of pulmonary tertiary lymphoid tissues and anti-nuclear antibodies following cessation of cigarette smoke exposure. *Respir Res.* 2014;15(1):49.

1110 33. Gray JP, and Hall GJ. In: Wexler P ed. *Encyclopedia of Toxicology (Third Edition).* Oxford:
1111 Academic Press; 2014:1050-1.
1112 34. Enzmann G, Adelfio R, Godel A, Haghayegh Jahromi N, Tietz S, Burgener SS, Deutsch U, Wekerle
1113 H, Benarafa C, and Engelhardt B. The Genetic Background of Mice Influences the Effects of
1114 Cigarette Smoke on Onset and Severity of Experimental Autoimmune Encephalomyelitis. *Int J*
1115 *Mol Sci.* 2019;20(6).
1116 35. Ho J, Koshibu K, Xia W, Luettich K, Kondylis A, Garcia L, Phillips B, Peitsch M, and Hoeng J. Effects
1117 of cigarette smoke exposure on a mouse model of multiple sclerosis. *Toxicol Rep.* 2022;9(597-
1118 610.
1119 36. Gao Z, Nissen JC, Ji K, and Tsirka SE. The experimental autoimmune encephalomyelitis disease
1120 course is modulated by nicotine and other cigarette smoke components. *PLoS One.*
1121 2014;9(9):e107979.
1122 37. Odoardi F, Sie C, Streyl K, Ulaganathan VK, Schlager C, Lodygin D, Heckelsmiller K, Nietfeld W,
1123 Ellwart J, Klinkert WE, et al. T cells become licensed in the lung to enter the central nervous
1124 system. *Nature.* 2012;488(7413):675-9.
1125 38. El-Behi M, Ciric B, Dai H, Yan Y, Cullimore M, Safavi F, Zhang GX, Dittel BN, and Rostami A. The
1126 encephalitogenicity of T(H)17 cells is dependent on IL-1- and IL-23-induced production of the
1127 cytokine GM-CSF. *Nature immunology.* 2011;12(6):568-75.
1128 39. Lee G, Jung KH, Shin D, Lee C, Kim W, Lee S, Kim J, and Bae H. Cigarette Smoking Triggers Colitis
1129 by IFN-gamma(+) CD4(+) T Cells. *Front Immunol.* 2017;8(1344.
1130 40. Qiu SL, Duan MC, Liang Y, Tang HJ, Liu GN, Zhang LM, and Yang CM. Cigarette Smoke Induction
1131 of Interleukin-27/WSX-1 Regulates the Differentiation of Th1 and Th17 Cells in a Smoking Mouse
1132 Model of Emphysema. *Front Immunol.* 2016;7(553.
1133 41. Ockinger J, Hagemann-Jensen M, Kullberg S, Engvall B, Eklund A, Grunewald J, Piehl F, Olsson T,
1134 and Wahlstrom J. T-cell activation and HLA-regulated response to smoking in the deep airways
1135 of patients with multiple sclerosis. *Clin Immunol.* 2016;169(114-20.
1136 42. Berer K, Mues M, Koutrolos M, Rasbi ZA, Boziki M, Johner C, Wekerle H, and Krishnamoorthy G.
1137 Commensal microbiota and myelin autoantigen cooperate to trigger autoimmune
1138 demyelination. *Nature.* 2011;479(7374):538-41.
1139 43. Krishnamoorthy G, Saxena A, Mars LT, Domingues HS, Mentele R, Ben-Nun A, Lassmann H,
1140 Dornmair K, Kurschus FC, Liblau RS, et al. Myelin-specific T cells also recognize neuronal
1141 autoantigen in a transgenic mouse model of multiple sclerosis. *Nat Med.* 2009;15(6):626-32.
1142 44. Botelho FM, Bauer CM, Finch D, Nikota JK, Zavitz CC, Kelly A, Lambert KN, Piper S, Foster ML,
1143 Goldring JJ, et al. IL-1alpha/IL-1R1 expression in chronic obstructive pulmonary disease and
1144 mechanistic relevance to smoke-induced neutrophilia in mice. *PloS one.* 2011;6(12):e28457.
1145 45. Botelho FM, Nikota JK, Bauer C, Davis NH, Cohen ES, Anderson IK, Coyle AJ, Kolbeck R, Humbles
1146 AA, Stampfli MR, et al. A mouse GM-CSF receptor antibody attenuates neutrophilia in mice
1147 exposed to cigarette smoke. *The European respiratory journal.* 2011;38(2):285-94.
1148 46. Morissette MC, Shen P, Thayaparan D, and Stampfli MR. Disruption of pulmonary lipid
1149 homeostasis drives cigarette smoke-induced lung inflammation in mice. *Eur Respir J.*
1150 2015;46(5):1451-60.
1151 47. Robbins CS, Bauer CM, Vujicic N, Gaschler GJ, Lichty BD, Brown EG, and Stampfli MR. Cigarette
1152 smoke impacts immune inflammatory responses to influenza in mice. *Am J Respir Crit Care Med.*
1153 2006;174(12):1342-51.
1154 48. Roos AB, Sethi S, Nikota J, Wrona CT, Dorrington MG, Sanden C, Bauer CM, Shen P, Bowdish D,
1155 Stevenson CS, et al. IL-17A and the Promotion of Neutrophilia in Acute Exacerbation of Chronic
1156 Obstructive Pulmonary Disease. *American journal of respiratory and critical care medicine.*
1157 2015;192(4):428-37.

1158 49. Havenar-Daughton C, Lindqvist M, Heit A, Wu JE, Reiss SM, Kendric K, Belanger S, Kasturi SP,
1159 Landais E, Akondy RS, et al. CXCL13 is a plasma biomarker of germinal center activity. *Proc Natl*
1160 *Acad Sci U S A.* 2016;113(10):2702-7.
1161 50. Kearley J, Silver JS, Sanden C, Liu Z, Berlin AA, White N, Mori M, Pham TH, Ward CK, Criner GJ, et
1162 al. Cigarette smoke silences innate lymphoid cell function and facilitates an exacerbated type I
1163 interleukin-33-dependent response to infection. *Immunity.* 2015;42(3):566-79.
1164 51. Rothfuchs AG, Egen JG, Feng CG, Antonelli LR, Bafica A, Winter N, Locksley RM, and Sher A. In
1165 situ IL-12/23p40 production during mycobacterial infection is sustained by CD11bhigh dendritic
1166 cells localized in tissue sites distinct from those harboring bacilli. *J Immunol.* 2009;182(11):6915-
1167 25.
1168 52. Teng MW, Bowman EP, McElwee JJ, Smyth MJ, Casanova JL, Cooper AM, and Cua DJ. IL-12 and
1169 IL-23 cytokines: from discovery to targeted therapies for immune-mediated inflammatory
1170 diseases. *Nat Med.* 2015;21(7):719-29.
1171 53. Khader SA, Pearl JE, Sakamoto K, Gilmartin L, Bell GK, Jelley-Gibbs DM, Ghilardi N, deSauvage F,
1172 and Cooper AM. IL-23 compensates for the absence of IL-12p70 and is essential for the IL-17
1173 response during tuberculosis but is dispensable for protection and antigen-specific IFN-gamma
1174 responses if IL-12p70 is available. *J Immunol.* 2005;175(2):788-95.
1175 54. Mondal S, Roy A, and Pahan K. Functional blocking monoclonal antibodies against IL-12p40
1176 homodimer inhibit adoptive transfer of experimental allergic encephalomyelitis. *J Immunol.*
1177 2009;182(8):5013-23.
1178 55. Ponomarev ED, Shriver LP, Maresz K, Pedras-Vasconcelos J, Verthelyi D, and Dittel BN. GM-CSF
1179 production by autoreactive T cells is required for the activation of microglial cells and the onset
1180 of experimental autoimmune encephalomyelitis. *J Immunol.* 2007;178(1):39-48.
1181 56. Segal BM, Constantinescu CS, Raychaudhuri A, Kim L, Fidelus-Gort R, Kasper LH, and
1182 Ustekinumab MSI. Repeated subcutaneous injections of IL12/23 p40 neutralising antibody,
1183 ustekinumab, in patients with relapsing-remitting multiple sclerosis: a phase II, double-blind,
1184 placebo-controlled, randomised, dose-ranging study. *Lancet Neurol.* 2008;7(9):796-804.
1185 57. Codarri L, Gyulveszi G, Tosevski V, Hesske L, Fontana A, Magnenat L, Suter T, and Becher B.
1186 RORgammat drives production of the cytokine GM-CSF in helper T cells, which is essential for
1187 the effector phase of autoimmune neuroinflammation. *Nat Immunol.* 2011;12(6):560-7.
1188 58. Komuczki J, Tuzlak S, Friebel E, Hartwig T, Spath S, Rosenstiel P, Waisman A, Opitz L, Oukka M,
1189 Schreiner B, et al. Fate-Mapping of GM-CSF Expression Identifies a Discrete Subset of
1190 Inflammation-Driving T Helper Cells Regulated by Cytokines IL-23 and IL-1beta. *Immunity.*
1191 2019;50(5):1289-304 e6.
1192 59. Hedstrom AK, Bomfim IL, Barcellos LF, Briggs F, Schaefer C, Kockum I, Olsson T, and Alfredsson L.
1193 Interaction between passive smoking and two HLA genes with regard to multiple sclerosis risk.
1194 *Int J Epidemiol.* 2014;43(6):1791-8.
1195 60. Xu W, Li R, and Sun Y. Increased IFN-gamma-producing Th17/Th1 cells and their association with
1196 lung function and current smoking status in patients with chronic obstructive pulmonary
1197 disease. *BMC Pulm Med.* 2019;19(1):137.
1198 61. Brozyna S, Ahern J, Hodge G, Nairn J, Holmes M, Reynolds PN, and Hodge S. Chemotactic
1199 mediators of Th1 T-cell trafficking in smokers and COPD patients. *COPD.* 2009;6(1):4-16.
1200 62. Shan M, Cheng HF, Song LZ, Roberts L, Green L, Hacken-Bitar J, Huh J, Bakaeen F, Coxson HO,
1201 Storness-Bliss C, et al. Lung myeloid dendritic cells coordinately induce TH1 and TH17 responses
1202 in human emphysema. *Science translational medicine.* 2009;1(4):4ra10.
1203 63. Shan M, Yuan X, Song LZ, Roberts L, Zarinkamar N, Seryshev A, Zhang Y, Hilsenbeck S, Chang SH,
1204 Dong C, et al. Cigarette smoke induction of osteopontin (SPP1) mediates T(H)17 inflammation in
1205 human and experimental emphysema. *Science translational medicine.* 2012;4(117):117ra9.

1206 64. Liang C, Shen Y, Xu Y, Liang Y, Qiu S, Tang H, and Zhong X. Dendritic Cells Promote the
1207 Differentiation of ILCs into NCR(-)ILC3s in the Lungs of Mice Exposed to Cigarette Smoke. *Copd.*
1208 2024;21(1):2389909.
1209 65. Naessens T, Morias Y, Hamrud E, Gehrmann U, Budida R, Mattsson J, Baker T, Skogberg G,
1210 Israelsson E, Thorn K, et al. Human Lung Conventional Dendritic Cells Orchestrate Lymphoid
1211 Neogenesis during Chronic Obstructive Pulmonary Disease. *American journal of respiratory and*
1212 *critical care medicine.* 2020;202(4):535-48.
1213 66. Grifka-Walk HM, Giles DA, and Segal BM. IL-12-polarized Th1 cells produce GM-CSF and induce
1214 EAE independent of IL-23. *Eur J Immunol.* 2015;45(10):2780-6.
1215 67. Mondal S, Kundu M, Jana M, Roy A, Rangasamy SB, Modi KK, Wallace J, Albalawi YA, Balabanov
1216 R, and Pahan K. IL-12 p40 monomer is different from other IL-12 family members to selectively
1217 inhibit IL-12Rbeta1 internalization and suppress EAE. *Proc Natl Acad Sci U S A.*
1218 2020;117(35):21557-67.
1219 68. Guo DH, Yamamoto M, Hernandez CM, Khodadadi H, Baban B, and Stranahan AM. Visceral
1220 adipose NLRP3 impairs cognition in obesity via IL-1R1 on CX3CR1+ cells. *J Clin Invest.*
1221 2020;130(4):1961-76.
1222 69. Tian X, Wang S, Zhang C, Prakash YS, and Vassallo R. Blocking IL-23 Signaling Mitigates Cigarette
1223 Smoke-Induced Murine Emphysema. *Environ Toxicol.* 2024;39(12):5334-46.
1224 70. Khader SA, Partida-Sanchez S, Bell G, Jelley-Gibbs DM, Swain S, Pearl JE, Ghilardi N, Desauvage
1225 FJ, Lund FE, and Cooper AM. Interleukin 12p40 is required for dendritic cell migration and T cell
1226 priming after Mycobacterium tuberculosis infection. *The Journal of experimental medicine.*
1227 2006;203(7):1805-15.
1228 71. Cua DJ, Sherlock J, Chen Y, Murphy CA, Joyce B, Seymour B, Lucian L, To W, Kwan S, Churakova
1229 T, et al. Interleukin-23 rather than interleukin-12 is the critical cytokine for autoimmune
1230 inflammation of the brain. *Nature.* 2003;421(6924):744-8.
1231 72. Segal BM, Dwyer BK, and Shevach EM. An interleukin (IL)-10/IL-12 immunoregulatory circuit
1232 controls susceptibility to autoimmune disease. *J Exp Med.* 1998;187(4):537-46.
1233 73. Blanquart E, Mandonnet A, Mars M, Cenac C, Anesi N, Mercier P, Audouard C, Roga S, Serrano
1234 de Almeida G, Bevan CL, et al. Targeting androgen signaling in ILC2s protects from IL-33-driven
1235 lung inflammation, independently of KLRG1. *The Journal of allergy and clinical immunology.*
1236 2022;149(1):237-51 e12.
1237 74. Bal SM, Bernink JH, Nagasawa M, Groot J, Shikhagaie MM, Golebski K, van Drunen CM, Lutter R,
1238 Jonkers RE, Hombrink P, et al. IL-1beta, IL-4 and IL-12 control the fate of group 2 innate
1239 lymphoid cells in human airway inflammation in the lungs. *Nat Immunol.* 2016;17(6):636-45.
1240 75. Singh D, Guller P, Reid F, Doffman S, Seppala U, Psallidas I, Moate R, Smith R, Kiraga J, Jimenez E,
1241 et al. A phase 2a trial of the IL-33 mAb tozorakimab in patients with COPD: FRONTIER-4. *The*
1242 *European respiratory journal.* 2025.
1243 76. Faiz A, Mahbub RM, Boedijono FS, Tomassen MI, Kooistra W, Timens W, Nawijn M, Hansbro PM,
1244 Johansen MD, Pouwels SD, et al. IL-33 Expression Is Lower in Current Smokers at both
1245 Transcriptomic and Protein Levels. *Am J Respir Crit Care Med.* 2023;208(10):1075-87.
1246 77. Blackmore S, Hernandez J, Juda M, Ryder E, Freund GG, Johnson RW, and Steelman AJ. Influenza
1247 infection triggers disease in a genetic model of experimental autoimmune encephalomyelitis.
1248 *Proc Natl Acad Sci U S A.* 2017;114(30):E6107-E16.
1249 78. Kronzer VL, Huang W, Dellaripa PF, Huang S, Feathers V, Lu B, Iannaccone CK, Gill RR, Hatabu H,
1250 Nishino M, et al. Lifestyle and Clinical Risk Factors for Incident Rheumatoid Arthritis-associated
1251 Interstitial Lung Disease. *J Rheumatol.* 2021;48(5):656-63.

79. Buljevac D, Flach HZ, Hop WC, Hijdra D, Laman JD, Savelkoul HF, van Der Meche FG, van Doorn PA, and Hintzen RQ. Prospective study on the relationship between infections and multiple sclerosis exacerbations. *Brain.* 2002;125(Pt 5):952-60.
80. Kriesel JD, White A, Hayden FG, Spruance SL, and Petajan J. Multiple sclerosis attacks are associated with picornavirus infections. *Mult Scler.* 2004;10(2):145-8.
81. Sibley WA, Bamford CR, and Clark K. Clinical viral infections and multiple sclerosis. *Lancet.* 1985;1(8441):1313-5.
82. Panitch HS. Influence of infection on exacerbations of multiple sclerosis. *Ann Neurol.* 1994;36 Suppl(Suppl):S25-8.
83. Edwards S, Zvartau M, Clarke H, Irving W, and Blumhardt LD. Clinical relapses and disease activity on magnetic resonance imaging associated with viral upper respiratory tract infections in multiple sclerosis. *J Neurol Neurosurg Psychiatry.* 1998;64(6):736-41.
84. Tremlett H, van der Mei IA, Pittas F, Blizzard L, Paley G, Mesaros D, Woodbaker R, Nunez M, Dwyer T, Taylor BV, et al. Monthly ambient sunlight, infections and relapse rates in multiple sclerosis. *Neuroepidemiology.* 2008;31(4):271-9.
85. Marrie RA, Wolfson C, Sturkenboom MC, Gout O, Heinzlef O, Roullet E, and Abenhaim L. Multiple sclerosis and antecedent infections: a case-control study. *Neurology.* 2000;54(12):2307-10.
86. Chen Q, Liu Y, Lu A, Ni K, Xiang Z, Wen K, and Tu W. Influenza virus infection exacerbates experimental autoimmune encephalomyelitis disease by promoting type I T cells infiltration into central nervous system. *J Autoimmun.* 2017;77(1-10.
87. Hosang L, Canals RC, van der Flier FJ, Hollensteiner J, Daniel R, Flugel A, and Odoardi F. The lung microbiome regulates brain autoimmunity. *Nature.* 2022;603(7899):138-44.
88. Saito E, Gurczynski SJ, Kramer KR, Wilke CA, Miller SD, Moore BB, and Shea LD. Modulating lung immune cells by pulmonary delivery of antigen-specific nanoparticles to treat autoimmune disease. *Sci Adv.* 2020;6(42).
89. Rubin RL, Hermanson TM, Bedrick EJ, McDonald JD, Burchiel SW, Reed MD, and Sibbitt WL, Jr. Effect of cigarette smoke on autoimmunity in murine and human systemic lupus erythematosus. *Toxicol Sci.* 2005;87(1):86-96.

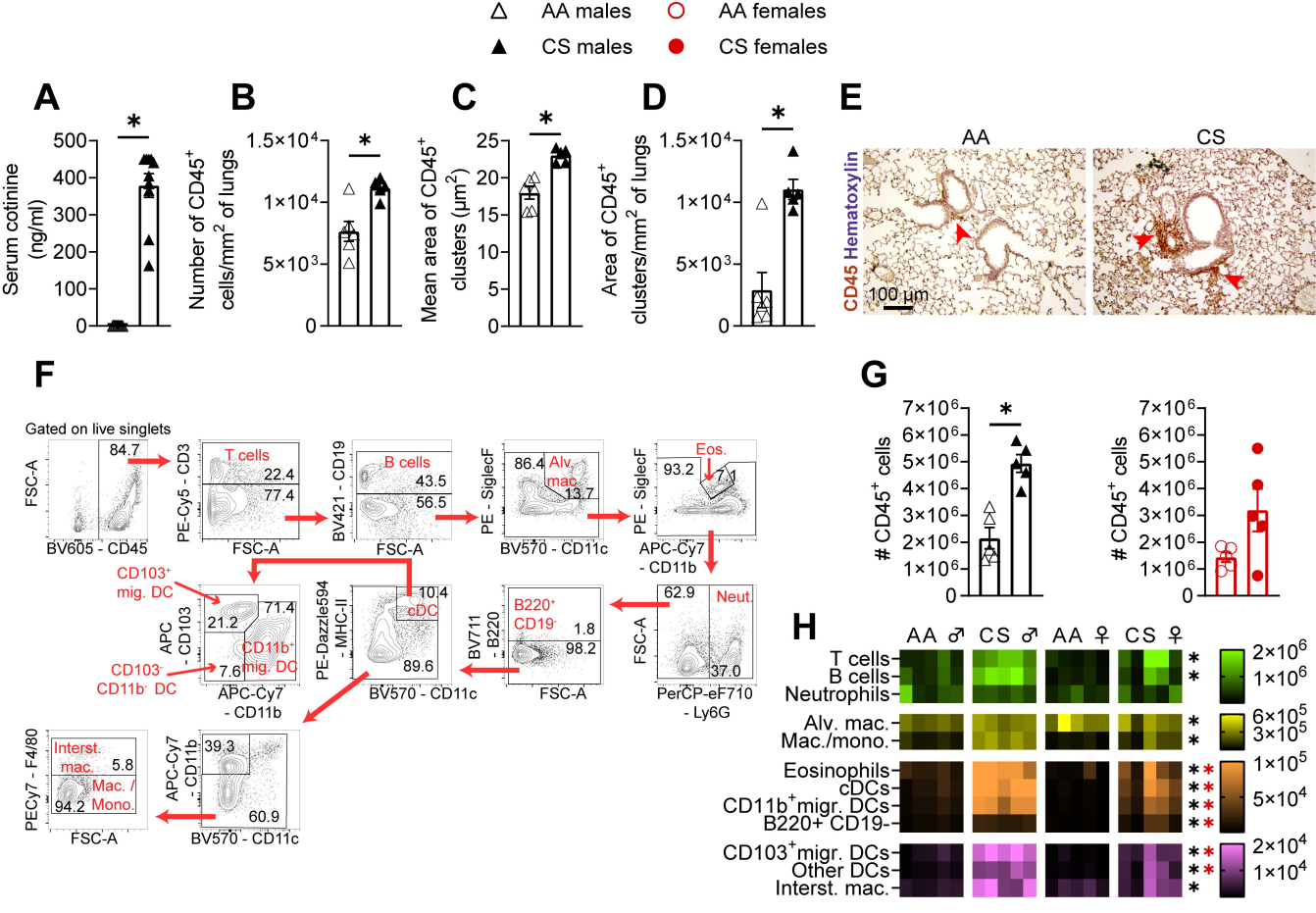
AA males
AA females
CS males
CS females
A
Serum cotinine (ng/ml)
B
Number of CD45+ cells/mm2 of lungs
C
Mean area of CD45+ clusters (μm2)
D
Area of CD45+ clusters/mm2 of lungs
E
AA
CS
CD45 Hematoxylin
100 μm
F
Gated on live singlets
T cells
B cells
Alv. mac.
Eos.
Neut.
CD103+ mig. DC
CD103- CD11b- DC
CD11b+ mig. DC
cDC
B220+ CD19-
Interst. mac.
Mac. / Mono.
G
CD45+ cells
H
AA ♂
CS ♂
AA ♀
CS ♀
T cells
B cells
Neutrophils
Alv. mac.
Mac./mono.
Eosinophils
cDCs
CD11b+migr. DCs
B220+ CD19-
CD103+migr. DCs
Other DCs
Interst. mac.

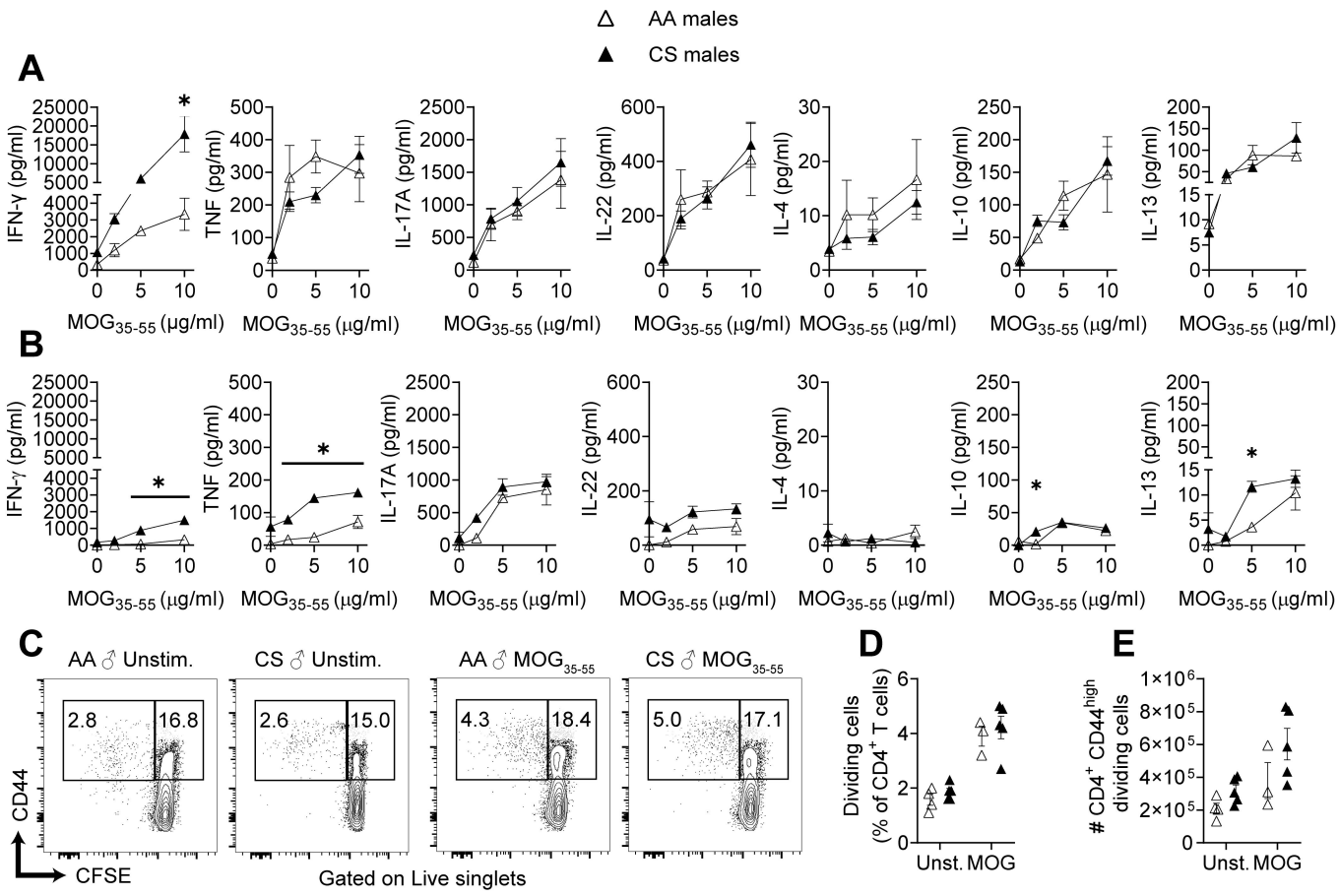
AA males
CS males
A
B
C
D
E
IFN-γ (pg/ml)
TNF (pg/ml)
IL-17A (pg/ml)
IL-22 (pg/ml)
IL-4 (pg/ml)
IL-10 (pg/ml)
IL-13 (pg/ml)
MOG35-55 (μg/ml)
AA ♂ Unstim.
CS ♂ Unstim.
AA ♂ MOG35-55
CS ♂ MOG35-55
2.8
16.8
2.6
15.0
4.3
18.4
5.0
17.1
CD44
CFSE
Gated on Live singlets
Dividing cells (% of CD4+ T cells)
CD44+ CD44high dividing cells
Unst.
MOG

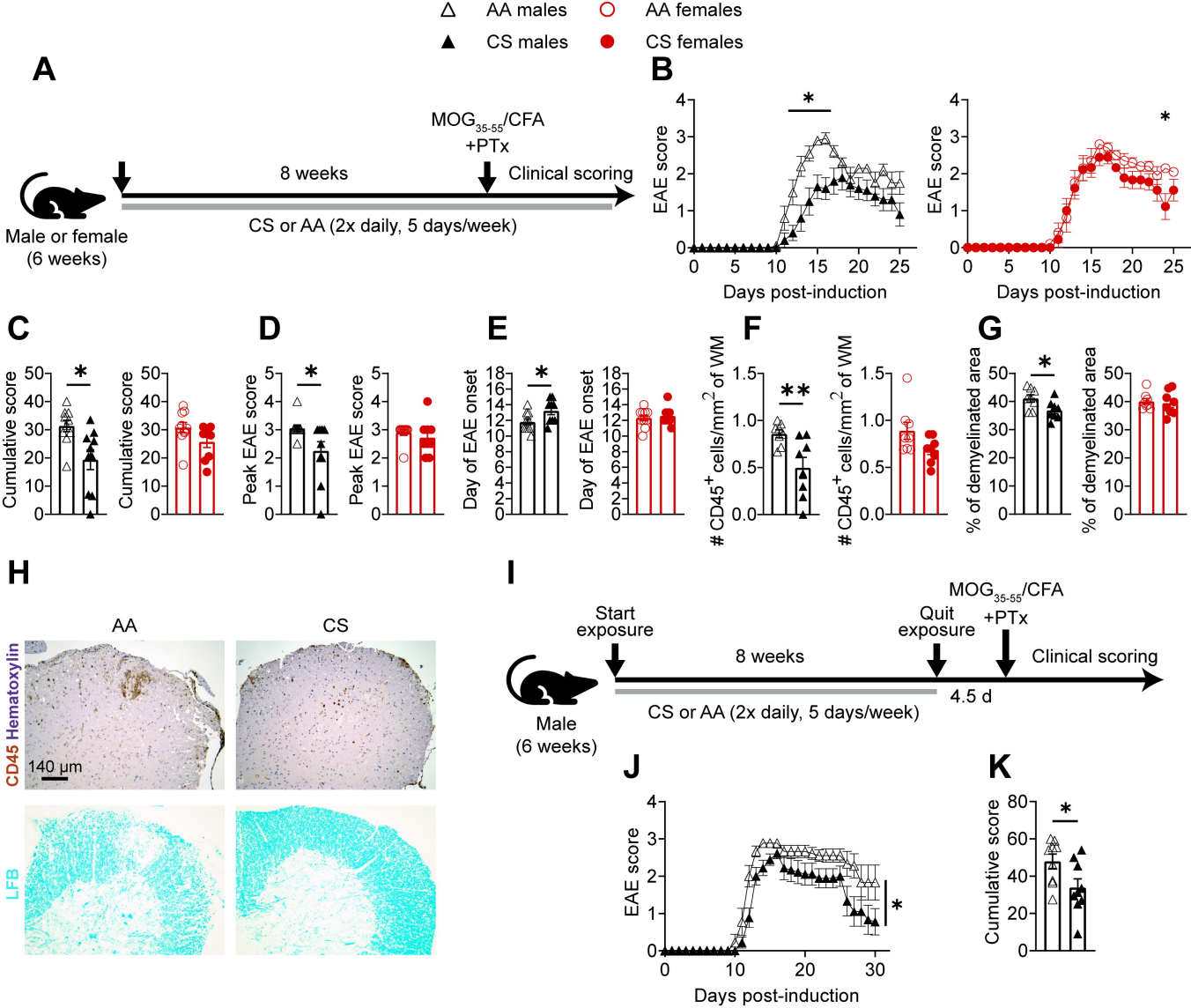
AA males
AA females
CS males
CS females
A
Male or female
(6 weeks)
8 weeks
MOG35-55/CFA
+PTx
Clinical scoring
CS or AA (2x daily, 5 days/week)
B
EAE score
Days post-induction
C
Cumulative score
D
Peak EAE score
E
Day of EAE onset
F
CD45+ cells/mm2 of WM
G
% of demyelinated area
H
AA
CS
CD45 Hematoxylin
LFB
140 µm
I
Start
exposure
Quit
exposure
MOG35-55/CFA
+PTx
Clinical scoring
4.5 d
Male
(6 weeks)
J
K

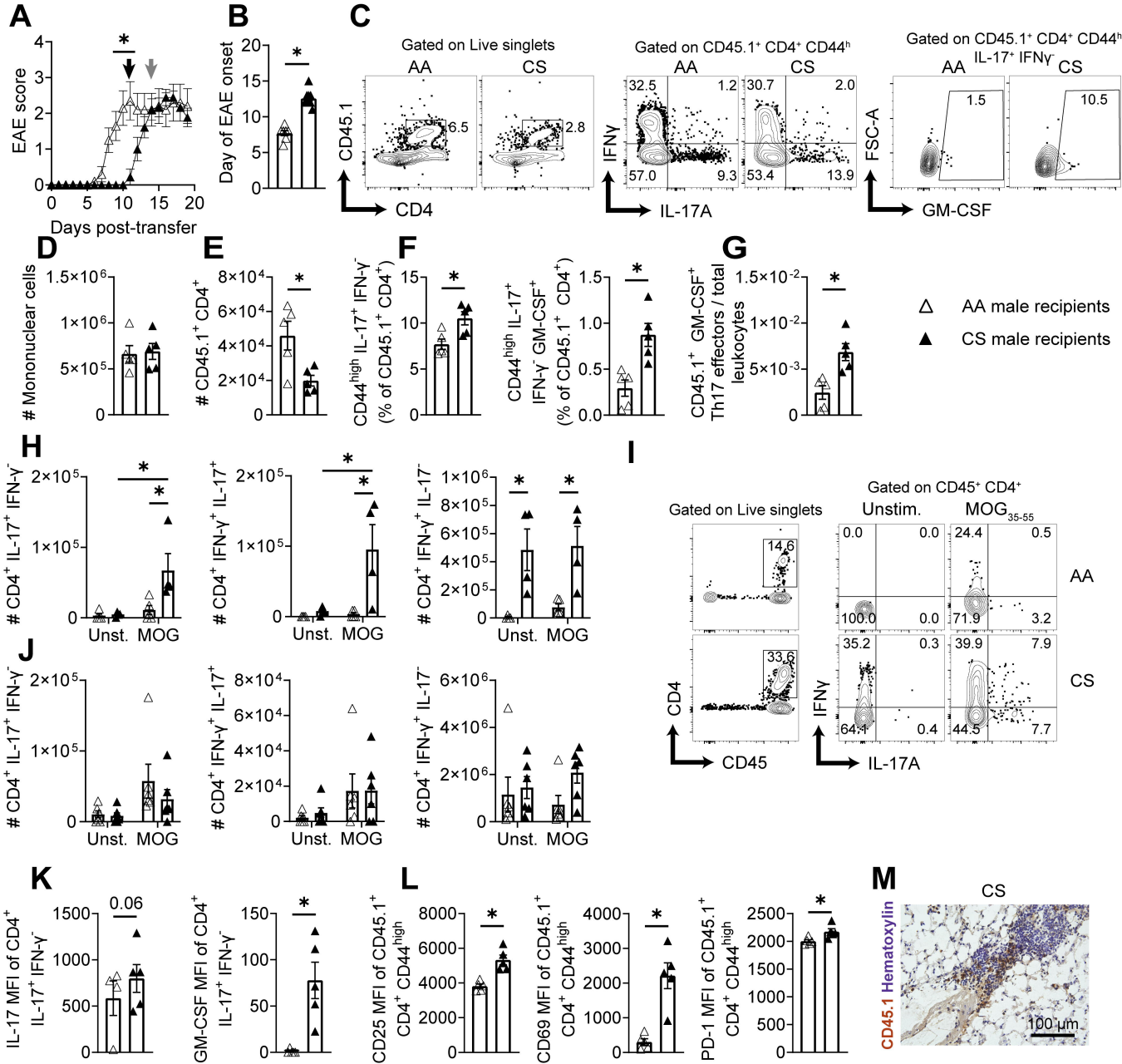
A
EAE score
Days post-transfer
B
Day of EAE onset
C
Gated on Live singlets
AA
CS
CD45.1
CD4
Gated on CD45.1+ CD4+ CD44h
IFNγ
IL-17A
Gated on CD45.1+ CD4+ CD44h IL-17+ IFNγ-
FSC-A
GM-CSF
D
Mononuclear cells
E
CD45.1+ CD4+
F
CD44high IL-17+ IFN-γ- (% of CD45.1+ CD4+)
CD44high IL-17+ IFN-γ- GM-CSF+ (% of CD45.1+ CD4+)
G
CD45.1+ GM-CSF+ Th17 effectors / total leukocytes
AA male recipients
CS male recipients
H
CD4+ IL-17+ IFN-γ-
CD4+ IFN-γ+ IL-17+
CD4+ IFN-γ+ IL-17-
Unst.
MOG
I
Gated on Live singlets
Gated on CD45+ CD4+
Unstim.
MOG35-55
CD45
J
K
IL-17 MFI of CD4+ IL-17+ IFN-γ-
GM-CSF MFI of CD4+ IL-17+ IFN-γ-
L
CD25 MFI of CD45.1+ CD4+ CD44high
CD69 MFI of CD45.1+ CD4+ CD44high
PD-1 MFI of CD45.1+ CD4+ CD44high
M
CS
CD45.1 Hematoxylin
100 µm

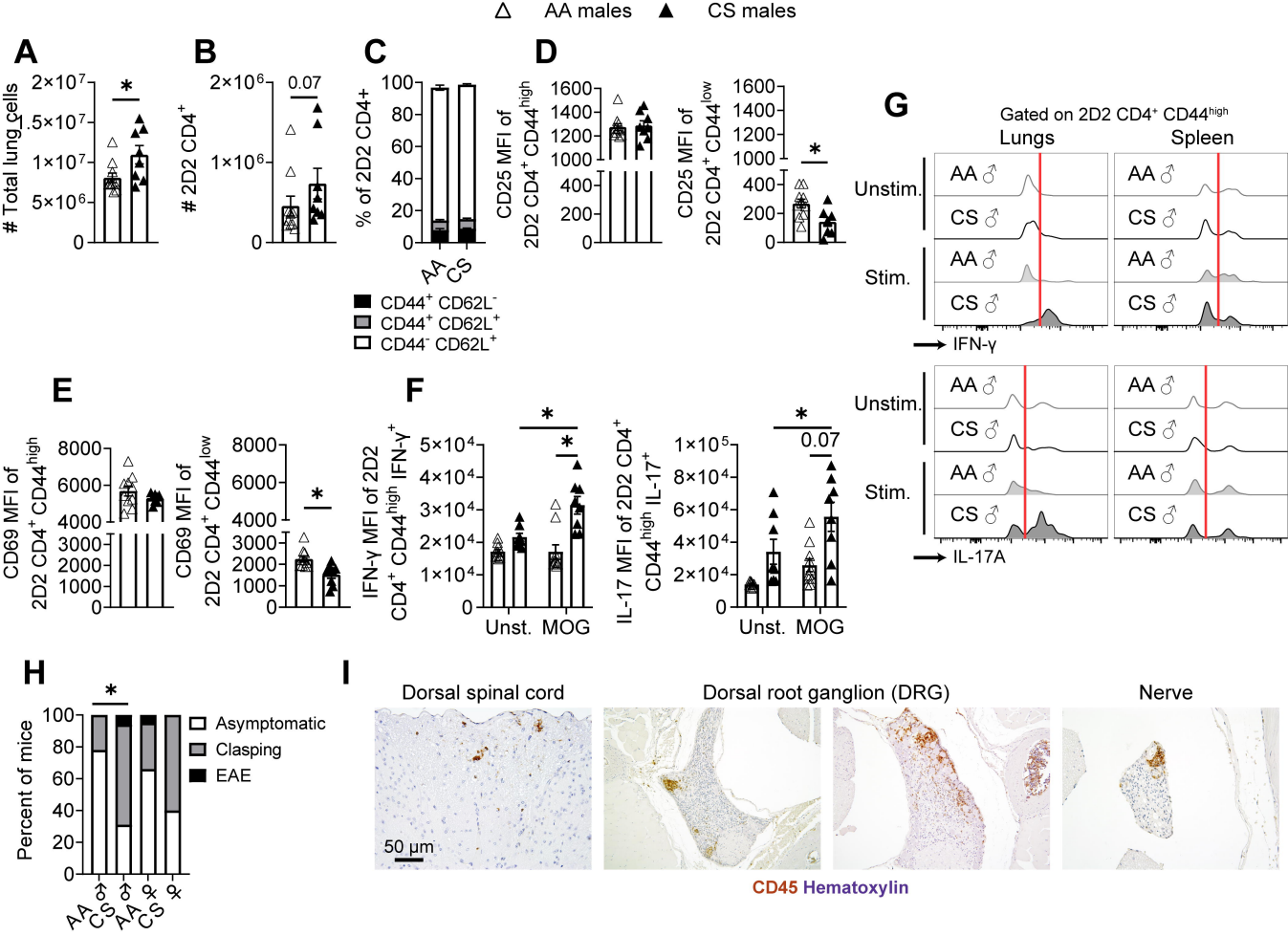
△ AA males ▲ CS males
A
Total lung cells
2×10^7
1.5×10^7
1×10^7
5×10^6
0
*
B
2D2 CD4+
2×10^6
1×10^6
0
0.07
C
% of 2D2 CD4+
100
80
60
40
20
0
AA
CS
CD44+ CD62L-
CD44+ CD62L+
CD44- CD62L+
D
CD25 MFI of 2D2 CD4+ CD44high
1600
1400
1200
1000
400
200
0
CD25 MFI of 2D2 CD4+ CD44low
*
G
Gated on 2D2 CD4+ CD44high
Lungs
Spleen
Unstim.
Stim.
AA ♂
CS ♂
IFN-γ
IL-17A
E
CD69 MFI of 2D2 CD4+ CD44high
8000
6000
4000
3000
2000
1000
0
CD69 MFI of 2D2 CD4+ CD44low
*
F
IFN-γ MFI of 2D2 CD4+ CD44high IFN-γ+
5×10^4
4×10^4
3×10^4
2×10^4
1×10^4
0
*
*
Unst.
MOG
IL-17 MFI of 2D2 CD4+ CD44high IL-17+
1×10^5
8×10^4
6×10^4
4×10^4
2×10^4
0
*
0.07
Unst.
MOG
H
Percent of mice
100
80
60
40
20
0
*
Asymptomatic
Clasping
EAE
AA
CS
AA
CS
♂
♂
♀
♀
I
Dorsal spinal cord
Dorsal root ganglion (DRG)
Nerve
50 µm
CD45 Hematoxylin

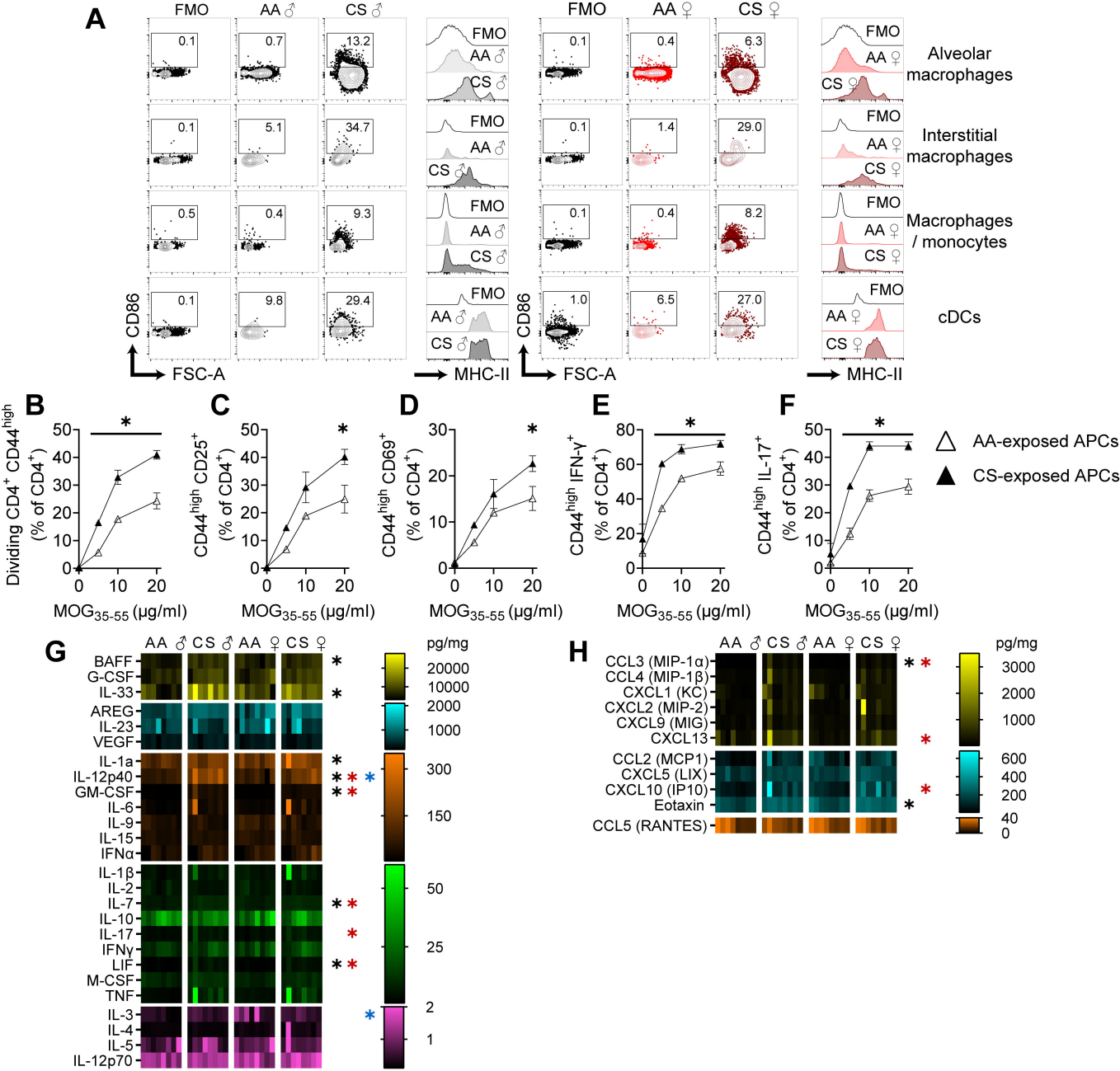
A
FMO
AA ♂
CS ♂
AA ♀
CS ♀
Alveolar macrophages
Interstitial macrophages
Macrophages / monocytes
cDCs
CD86
FSC-A
MHC-II
B
C
D
E
F
Dividing CD4+ CD44high (% of CD4+)
CD44high CD25+ (% of CD4+)
CD44high CD69+ (% of CD4+)
CD44high IFN-γ+ (% of CD4+)
CD44high IL-17+ (% of CD4+)
MOG35-55 (μg/ml)
AA-exposed APCs
CS-exposed APCs
G
H
pg/mg
BAFF
G-CSF
IL-33
AREG
IL-23
VEGF
IL-1a
IL-12p40
GM-CSF
IL-6
IL-9
IL-15
IFNα
IL-1β
IL-2
IL-7
IL-10
IL-17
IFNγ
LIF
M-CSF
TNF
IL-3
IL-4
IL-5
IL-12p70
CCL3 (MIP-1α)
CCL4 (MIP-1β)
CXCL1 (KC)
CXCL2 (MIP-2)
CXCL9 (MIG)
CXCL13
CCL2 (MCP1)
CXCL5 (LIX)
CXCL10 (IP10)
Eotaxin
CCL5 (RANTES)

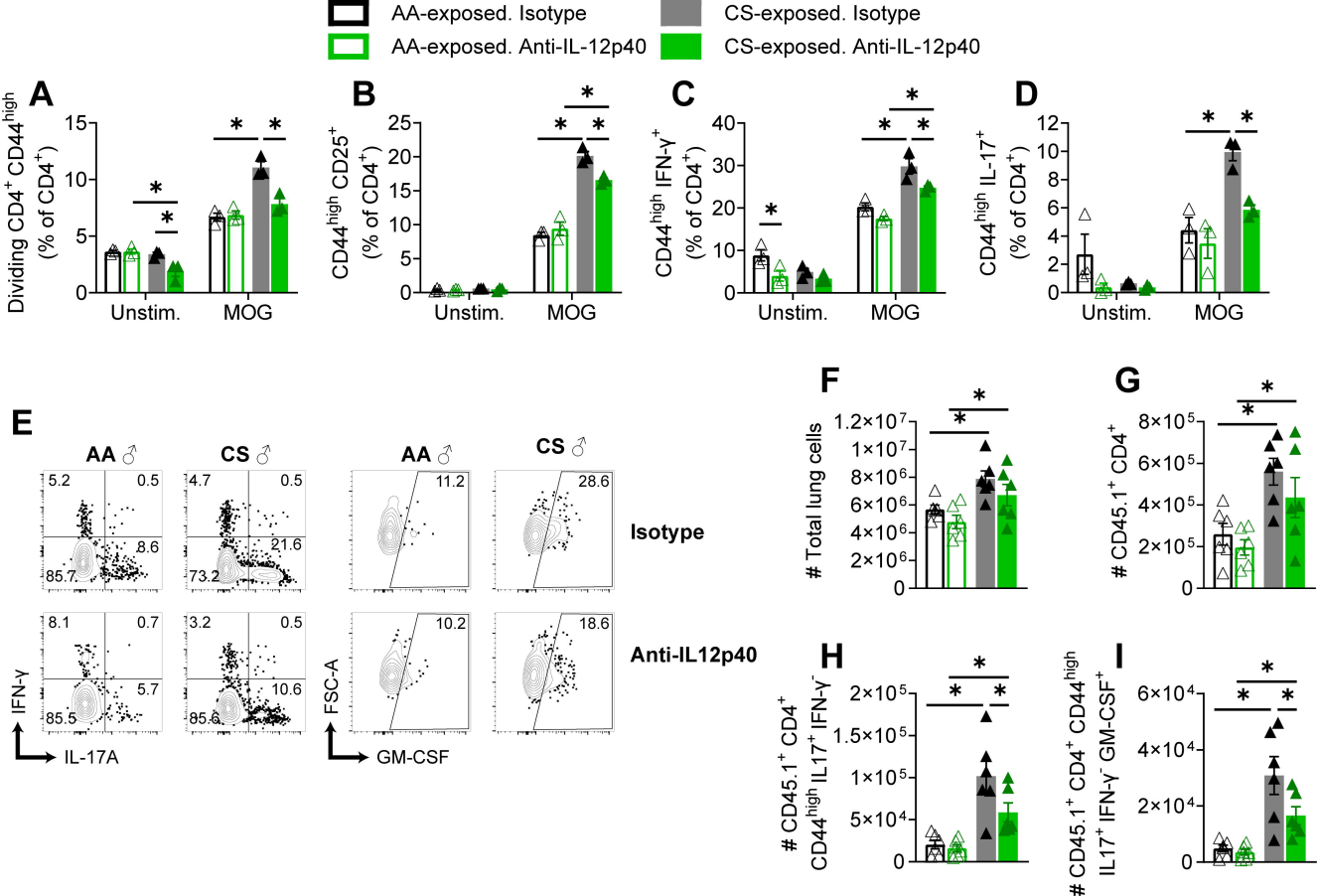
AA-exposed. Isotype
AA-exposed. Anti-IL-12p40
CS-exposed. Isotype
CS-exposed. Anti-IL-12p40
A
Dividing CD4+ CD44high (% of CD4+)
Unstim.
MOG
B
CD44high CD25+ (% of CD4+)
C
CD44high IFN-γ+ (% of CD4+)
D
CD44high IL-17+ (% of CD4+)
E
AA ♂
CS ♂
Isotype
Anti-IL12p40
IFN-γ
IL-17A
FSC-A
GM-CSF
F
Total lung cells
G
CD45.1+ CD4+
H
CD45.1+ CD4+ CD44high IL17+ IFN-γ-
I
CD45.1+ CD4+ CD44high IL17+ IFN-γ- GM-CSF+